Neural and Musculoskeletal Modeling: Its Role in Neurorehabilitation

M. Ali Akhras, Roberto Bortoletto, Forough Madehkhaksar and Luca Tagliapietra

Abstract Human NeuroMusculoSkeletal systems (NMS SYs) are very complex and have redundant anatomical degrees of freedom (DOFs) at muscles and joints. These features enable them to easily perform dexterous tasks since the childhood. NMS SYs have attracted many researchers from different scientific domains such as neurophysiology, robotics, biomechanics, and neuro-rehabilitation engineering because of its multi-task functionalities. Humans can perform hundreds of tasks and dynamically interact with external environments in a very efficient way without thinking about the complexity of the motor task. Thinking about twirling a coin or writing tasks, the many complex operations needed to perform such actions rise important questions like "do we really perform very complex computations to control our musculoskeletal system?" or "how do we control our musculoskeletal system to perform such actions?" and "what is the main contribution of our biomechanical structure in the motor control task?". Recently, scientists have paid more attention not only to the neural commands but also to the biomechanical properties of NMS Sys and their role in simplifying the motor control tasks. Muscles are the main building blocks in our biomechanical systems. They can be continuously co-activated to produce and to coordinate movements maintaining the stability. Muscle-tendon actuators have been physically modeled, based on Hill-Type model, to study their non-linear behaviors

M.A. Akhras (✉)
Department of Robotics, Brain, and Cognition Sciences, Istituto Italiano di Tecnologia, Genova, Italy
e-mail: ali.akhras@iit.it

R. Bortoletto
Intelligent Autonomous Systems Laboratory, Department of Information Engineering, University of Padova, Padova, Italy
e-mail: roberto.bortoletto@dei.unipd.it

F. Madehkhaksar
Department of Information and Computing Science, Utrecht University, Utrecht, Netherlands
e-mail: F.Madehkhaksar@uu.nl

L. Tagliapietra
Rehabilitation Engineering Group, Department of Management and Engineering, University of Padova, Padova, Italy
e-mail: tagliapietra@gest.unipd.it

J.L. Pons et al. (eds.), *Emerging Therapies in Neurorehabilitation II*,
Biosystems & Biorobotics 10, DOI 10.1007/978-3-319-24901-8_5

and characteristics. Those models were then integrated with neuron models to provide a better understanding of the local control mechanism of a motor unit (e.g. spinal cord motor neuron and muscle-tendon actuator). Motor unit behaviors are observed through the muscle activity: the physiological process of converting an electrical stimulus to a mechanical response. This process is fundamental to muscle physiology, whereby the electrical stimulus is usually an action potential and the mechanical response is contraction. The transformation from Electromyographic (EMG) signal to muscle activation is not trivial and can occur through several steps. Muscle activation dynamics is the physiological process described by those steps. In general, the control of NMS models can be achieved also by combining together the EMG signals to retrieve muscle synergies. Apparently, humans use different motor control strategies to command their actions, some already exist in the Central Nervous System (CNS) with their birth and many others are developed and/or adapted during their life and gained experiences. However, both views of control strategies suggest a task dependency of the neural control. More details on description of muscle co-activation patterns based on the two views of the task dependent motor control strategies are provided in this chapter which will give an insight not only on a higher level of neural control but also at a lower level control of muscles in the CNS. Computational musculoskeletal models can provide an accurate knowledge of the physiological loading conditions on the skeletal system during human movements and allow quantifying factors that affect musculoskeletal functions, thus it can significantly improve clinical treatments in several orthopedics and neurological contexts. Every patient is different and possesses unique anatomical, neurological, and functional characteristics that may significantly affect optimal treatment of the patient. Therefore, personalized computational models of NMS systems can facilitate prediction of patient-specific functional outcome for different treatment designs and provide useful information for clinicians. Personalize computational models can be derived by generic models or subject-specific models with different levels of subject-specific details. In this chapter, we describe NMS systems in a bottom-up fashion. First we provide a deep insight on muscle contraction dynamics and musculoskeletal system properties. Then we discuss how a musculoskeletal system is locally driven by neuromuscular controls. Afterwards, we define how central motor commands are mapped through muscle synergies into low level controls. We discuss the two visions on the motor control strategies that CNS might use to perform motor control tasks and some related aspects inspired from neurorehabilitation studies and motor control experiments. Finally, we describe the importance and application of personalized subject-specific musculoskeletal modeling in neurorehabilitation.

Keywords Neuromusculoskeletal modeling · Muscle-driven simulations · Muscle-tendon activation · Model calibration and validation · Motor control · Muscle synergies · Muscle co-contraction

1 Musculo-Tendon Models and Parameters

The CNS generates neural commands to activate the muscles in order to control the human body movements. Subsequent forces produced by muscles are transmitted through tendons to the skeleton to perform a motor task. Thus, muscles and tendons are the interface between the CNS and the articulated body segments. A firm understanding of the properties of this framework is important to scientists in order interpret kinesiological events in the context of coordination of the body, and to engineers in order to design prosthetic, orthotic, and functional neuromuscular stimulation systems that helps to restore lost or impaired motor function. Biomechanical models have been used in several studies to predict muscle forces and joint torques along with human body motion. One of the first muscle's mathematical models was proposed by Hill [74]. Gordon et al. [66] refined such model by incorporating the dependence between changes in muscle force as function of muscle lengths and contraction speeds. Zajac extended the Hill's model introducing a muscle-tendon model [136], which is known as Hill-type muscle force model.

Hill-type muscle model is an important component of most of the adopted musculoskeletal models, yet it requires specific knowledge of several muscle and tendon properties. These include the Optimal Muscle Fibre Length (OMFL), the length at which the muscle can generate maximum force, and the Tendon Slack Length (TSL), the length at which the tendon starts to generate a resistive force to stretch. Both of these parameters extremely influence the force-generating behaviour of a musculotendon unit and vary with the size of the person. However, these properties are difficult to be directly measured in vivo and are often estimated using the results of cadaver studies, which do not account for differences in subject size [129]. The difficulty associated to the direct measurement of important variables, including the forces generated by muscles, is one of the main limitations related to the use of experiments only. As argued by Delp et al. [41], a theoretical framework is needed, in combination with experiments, to investigate the principles that govern the coordination of muscles during normal movement, to determine how neuromuscular impairments contribute to abnormal movement, and to predict the functional consequences of treatments. A dynamic simulation of movement that integrates models describing the anatomy and physiology of the elements of Neuromusculoskeletal (NMS) system and the mechanics of multijoint movement provides such a framework [41]. Muscle-driven simulations rely on computational models of musculotendon dynamics. These models are commonly subdivided into two classes: cross-bridge models [49, 72, 135] and Hill-type models [50, 131]. Although cross-bridge models have the advantage of being derived from the fundamental structure of muscle, they include many parameters that are difficult to measure and rarely used in muscle-driven simulations involving many muscles. For this reason and due to the fact that they are widely used in muscle-driven simulations thanks to their computational efficiency [2, 8, 13, 71, 78, 86, 118, 121, 137, 138], we focus here on Hill-type models.

1.1 Architecture of Muscle Tissue

Musculotendon actuators are assumed to be massless, frictionless, extensible strings that attach and wrap around bones and other structures [97]. Muscle are considered to be a collection of equally long coplanar fibers arranged in parallel, where all fibers are oriented either in the direction of the tendon or at an acute angle, also known as Pennation Angle (PA), $\alpha > 0$, to the tendon [136]. A common assumption is that muscle maintains a constant volume and the distance between the aponeurosis of origin and insertion is constant. The major effect on musculotendon function is that α increases as fibers shorten. Thus, muscle fibers shorten in a direction that is not colinear with the direction in which tendon stretches.

The length at which active muscle force peaks, L_0^M, is called OMFL. Notice that the shortest length at which passive muscle tissue develops force is L_0^M. Given the OMFL and the corresponding PA, α_0, at which the muscle develops the Maximum Isometric Force (MIF); the relationship between PA and Muscle Fiber Length (MFL), L^M, can be expressed as the following [62]:

$$\sin(\alpha) = \frac{L_0^M \sin(\alpha_0)}{L^M} \tag{1}$$

$$\cos(\alpha) = \sqrt{1 - \sin^2(\alpha)} = \sqrt{1 - \left(\frac{L_0^M \sin(\alpha_0)}{L^M}\right)^2} \tag{2}$$

For muscles with a small PA, the PA will have little effect on the force in the musculotendon unit. However, a large PA (i.e. greater than 20°) can have a significant effect on muscle force. PA can be directly derived from Eq. 1, at time t:

$$\alpha(t) = \sin^{-1}\left(\frac{L_0^M \sin(\alpha_0)}{L^M(t)}\right) \tag{3}$$

A muscle can be represented by n motor units being controlled by n nerve axons originating from the CNS, each with its own control $u_i(t)$. The muscle fibers of each motor unit i collectively develop a motor unit force F_i^M, which is most likely assumed to sum with the other motor unit forces to produce the net muscle force F^M. This assumption allows us to represent musculotendon actuators with a wide range of architectures with a single dimensionless model [14].

1.2 Hill-Type Muscle-Tendon Model

The general arrangement for a muscle-tendon model has a muscle fiber in series with an elastic or viscoelastic tendon (Fig. 1). The muscle fiber has a contractile component in parallel with an elastic component [25]. The Hill-type muscle model

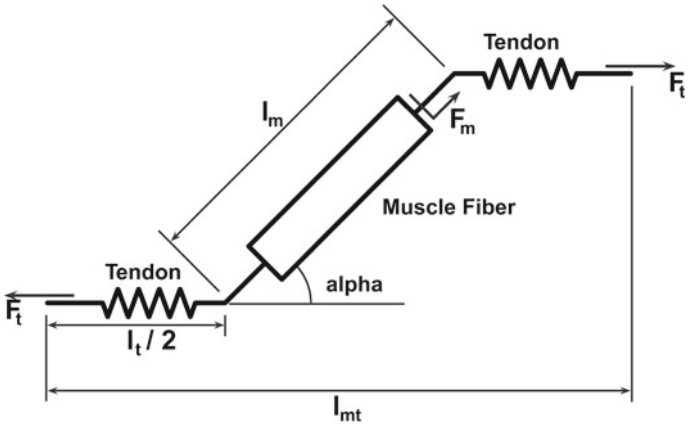

Fig. 1 Schematic of muscle-tendon unit showing muscle fibre in series with the tendon

is used to estimate the force that can be generated by the contractile element of the muscle fiber, using a Force-Length-Velocity (FLV) relation controlled by muscle activation. The general form of the function is given by:

$$F^M(t) = f(l)f(v)a(t)F_0^M \tag{4}$$

where $F^M(t)$ is the time varying muscle fiber force; $f(l)$ is the normalized length dependent fiber force; $f(v)$ is the normalized velocity dependent fiber force; $a(t)$ is the time varying muscle activation; and F_0^M is the MIF. Commonly, Hill's equation [74] is modified and used as an expression [16, 131], although nothing precludes the use of other expressions [73].

Muscles could be imagined having an active part which generates force when activated, like a motor, and an in-parallel passive part that applies a resistive force when stretched beyond a resting length, like a rubber band [25]. Sometimes a muscle elastic element, distinguishable from tendon elasticity is included in series with the active part, which is due to the contractile elements [136]. These yield a MIF when the sarcomeres are at an OMFL (i.e. when there is optimal overlap of the actin and myosin myofilaments). When the muscle length is above that optimal length, it cannot generate as much force because there is less actin-myosin overlap which reduces the force-generating potential of the muscle.

1.2.1 Force-Length Relation

The static property of muscle tissue is defined by its isometric Force-Length curve (FLc). This property can be studied when activation $a(t)$ and fiber length L^M are constant. Full activation ($a(t) = 1$) occurs when muscle tissue has been maximally excited ($u(t) = 1$). Conversely, muscle tissue that has been neither neurally nor

electrically excited for a long time is said to be passive ($u(t) = a(t) = 0$) [136]. MIF, F_0^M, is assumed to be proportional to Physiological Cross-Sectional Area (PCSA), where PCSA is defined as the ratio between muscle volume and OMFL:

$$PCSA = \frac{Volume}{L_0^M} \tag{5}$$

Typically, the volume of a muscle is calculated from its weight multiplied by the density of muscle tissue: 1.06 g/cm^3 [100]. The proportionality constant relating F_0^M to *PCSA* represents the Maximum Muscle Stress (MMS) [62].

The difference in force developed when muscle is activated and when muscle is passive is called Active Muscle Force (AMF), F_A^M.

$$F_A^M = f_A(l) F_0^m a(t) \tag{6}$$

where $a(t)$ is accounted for since the level of muscle activation determines the MIF produced by the muscle.

The muscle force-length is also coupled to the level of activation [70]. Lloyd and Besier [88] incorporated this coupling between activation and OMFL into the muscle-tendon model using the following relationship:

$$L_0^M(t) = L_0^M \left(\lambda \left(1 - a(t)\right) + 1\right) \tag{7}$$

The percentage change in OMFL defines how much the OMFL shifts to longer lengths, at time t and activation $a(t)$.

Mathematically, it is often more helpful to consider the force-length relationship in dimensionless units. Zajac [136] represented this property in terms of Normalized Muscle Force (NMF), $\tilde{F}^M$, and Normalized Muscle Fiber Length (NMFL), $\tilde{L}^M$.

$$\tilde{F}^M = F^M / F_0^M \tag{8}$$

$$\tilde{L}^M = L^M / L_0^M \tag{9}$$

As depicted in Fig. 2, the effective operating range of muscle begins at roughly $0.5L_0^M$ and ends at $1.5L_0^M$; muscle cannot generate active force beyond these lengths. Furthermore, when muscle is stretched to lengths greater than $1.2L_0^M$, it generates a significant amount of Passive Muscle Force (PMF), F_P^M. It is due to the elasticity of the tissue that is in parallel with the contractile element. Passive forces are very small when the muscle fibers are shorter than their OMFL, and rise greatly thereafter [117].

$$F_P^M = f_P(l) F_0^M \tag{10}$$

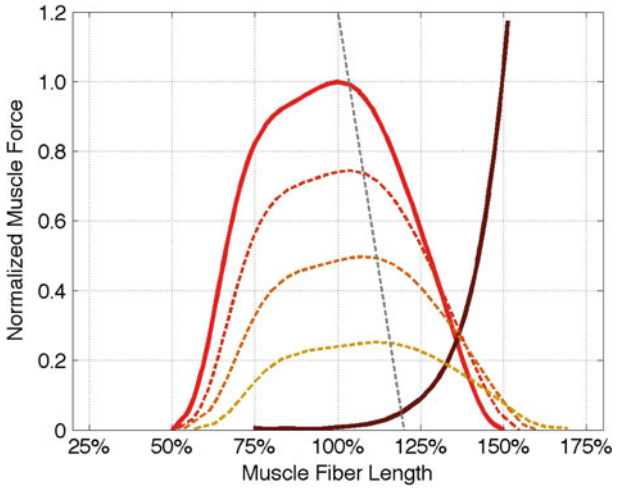

Fig. 2 Normalized forcelength relationship for muscle. Thick dark lines indicate maximum activation, whereas the light thin lines are lower levels of activation

The total normalized muscle force is the sum of the active and passive components, which can be scaled to different muscles to provide total isometric muscle force, F^M, by:

$$\begin{aligned} F^M &= \left[F_A^M + F_P^M\right]\cos(\alpha) \\ &= \left[f_A(l)a(t) + f_P(l)\right]F_0^M\cos(\alpha) \end{aligned} \tag{11}$$

It is also worth noting the importance of the fiber lengths operating range with respect to the required excursion of a muscle. Brand et al. [22] defined muscle excursion as the difference between the maximum physiological length, L_{max}^{MT}, and the minimum physiological length, L_{min}^{MT}, of the muscle: the extreme lengths of a musculotendon actuator when a joint is moved through its full range of motion. For muscles with a large excursion, one can expect the value of L_0^M to be relatively large; conversely, for muscles with a small excursion, the value of L_0^M should be relatively small. Unfortunately, the relationship between OMFL and musculotendon excursion has been shown to vary widely among muscles, and it cannot be used to define the value of L_0^M precisely. As discussed in [62], also the value of TSL, L_s^T, affects the relation between OMFL and musculotendon excursion. If we assume that the total length, L^{MT}, of a musculotendon actuator is given by the sum of muscle length, L^M, and tendon length, L^T, then the tendon length will affect the length of the muscle when the actuator is at L_{min}^{MT} and L_{max}^{MT}. If tendon is assumed to be sufficiently stiff so that a change in its length is negligible compared to a change in muscle length, then all variation in musculotendon length, L^{MT}, can be attributed to a change in muscle length. On the other hand, if an actuator has minimum and maximum physiological lengths which are both relatively large, then one can expect the value of TSL, L_s^T, to

be large and the value of OMFL, L_0^M, to be small. Conversely, if L_{min}^{MT} is relatively small, then L_s^T should be small and L_0^M should be large. It is clear that L_0^M, L_s^T, L_{min}^{MT}, and L_{max}^{MT} are all related.

1.2.2 Force-Velocity Relation

Muscle tissue is subject to a constant tension when it's fully activated. It first shortens then stops (i.e. isometric contraction). The length at which shortening terminates corresponds to the length at which such a force can be sustained in steady-state [136]. From a set of length trajectories, obtained by subjecting muscle to different tensions, a Force-Velocity relation can be constructed for any length L^M, where $0.5L_0^M < L^M < 1.5L_0^M$. Finally, at OMFL, L_0^M, a Maximum Shortening Velocity (MSV), v_0^M, can be defined from the Force-Velocity curve (FVc). At this velocity, muscle cannot sustain any tension, even when fully activated.

The shape of the FVc determines the mechanical power output that active muscle delivers. During shortening, muscle delivers power (power output is positive), with peak power output occuring when muscle shortens at about $0.3v_0^M$ [136]. The shape of FVc during lengthening is very important during computer simulation of movement. Common assumption are that (Fig. 3):

1. The FV relation scales with length and activation in one of two ways: either the velocity-axis intercept remains constant under all conditions or decreases with $a(t)$ and L^M);
2. No discontinuity in slope at F_0^M exists, even though experiments and cross-bridge theory suggest one;
3. The FVc at any instant is unaffected by preceding events, even though it is known that prestretched muscle tissue subsequently shortens faster.

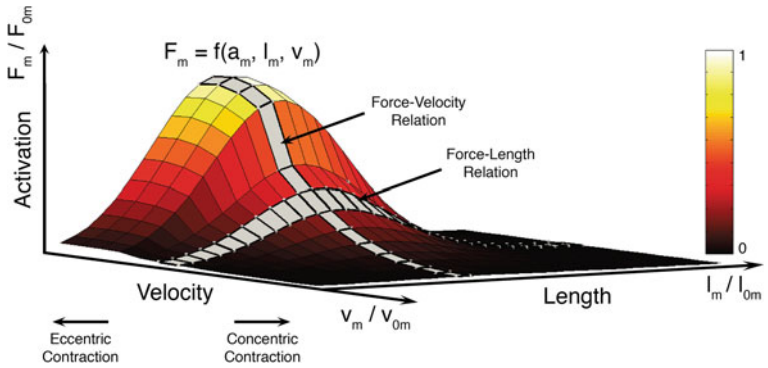

Fig. 3 The Active Force-Length-Velocity (FLV) surface of muscle is defined by the muscle's Optimal Fiber Length (OFL), Maximum Shortening Velocity (MSV), and Maximum Isometric Force (MIF). Active muscle force generation can be constrained to this surface and scaled by the level of muscle activation. Force-Length and Force-Velocity curves are highlighted in gray

MSV, v_0^M, is commonly defined as the number of OMFL per second, and it is treated as a constant. However, it could be varied depending on the relative fiber mixes in muscles. Yamaguchi et al. [134] listed the fiber mixture percentages to be considered as common starting point, but it is well known that people do have different fast-twitch to slow-twitch fiber ratios. A detailed discussion about the ways in which the force-length and force-velocity relationships could be most readily combined for shortening muscle can be found at [25].

Given a value of L^M, PA is calculated using Eq. 3. Subsequently, since the muscle-tendon length, L^{MT}, is a known input of the model (it is directly related to the musculotendon kinematics), the tendon lenght is computed as follows:

$$L^T = L^{MT} - L^M \cos(\alpha) \tag{12}$$

Once tendon length is established, also tendon force, F^T, can be determined (see Sect. 1.3). Given the total muscle force (Eq. 11), the corresponding normalized velocity dependent fiber force, $f(v)$, can be computed as follows:

$$f(v) = \frac{F^T - f_P(l) F_0^M \cos(\alpha)}{f_A(l) a(t) F_0^M \cos(\alpha)} \tag{13}$$

Once $f(v)$ is calculated, we can solve for fiber velocity, v^M.

1.3 Tendon Model

Tendons are commonly defined as a external portion to muscle passive elements that act like rubber bands. Tendons do not carry any load their length is below the TSL and generates a force proportional to the stretch distance if their length is above TSL. Given the tendon length, L^T, tendon strain (i.e. tendon stretch relative to its resting) can be defined as follows:

$$\varepsilon^T = \frac{L^T - L_s^T}{L_s^T} \tag{14}$$

Data suggest that the same strain is experienced throughout internal and external tendon. It is also convenient to assume that the Stress-Strain properties of external and internal tendon are the same, where the Tendon Stress, σ^T, is defined by the ratio of tendon force, F^T, to Tendon Cross-Sectional Area (TCSA), as follows:

$$\sigma^T = \frac{F^T}{TCSA} \tag{15}$$

Notice that the tendon force varies with the strain only when the tendon length is greater than the TSL, otherwise the tendon force is zero. Hence, tendon behavior can be modeled through a generic Force-Strain curve (FSc). As depicted in Fig. 4,

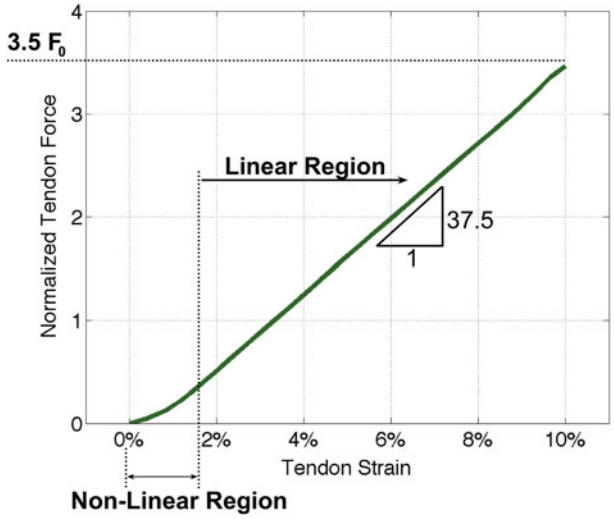

Fig. 4 Mechanical properties of tendon

the tendon tangent modulus of elasticity (i.e., the slope of the tendon stress-strain curve) increases with strain at low strains, and then is constant at higher strains until failure. Zajac [136] observed from the literature that the strain in tendon is 3.3 % when the muscle generates MIF, corresponding to a nominal value for σ_0^T of 32 MPa.

1.4 Musculo-Skeletal Kinematics

Once the muscle-tendon force is computed, it is important to compute the corresponding contribution to joint moment. This requires knowledge of the muscle's moment arm, r, which can be shown to be a function of the muscle's length [95]. To compute both the length and the moment arm for a musculotendon unit, a musculoskeletal model is required. Musculotendon kinematics estimations can be produced by a software that model the geometry of the bones, the complex relationships associated with joint kinematics, and the musculotendon paths wrapping around points and surfaces [41]. This is based on obstacle detection and may cause discontinuities in the predicted musculotendon kinematics [61]. On the other hand, it is desirable that musculotendon kinematics equations are continuously differentiable to enable the computation of analytical Jacobians for the forward simulation of the musculoskeletal system [2, 113].

Sets of differentiable polynomial regression equations have been proposed to estimate L^{MT} and r from nominal values of both parameters corresponding to combinations of discrete joint angles or Generalized Coordinates (GCs) [95]. This required gathering data sets on both L^{MT} and r and manually identifying the best-performing

equations that depended on the muscle, number of GCs, and the fitted musculotendon parameter. This necessitated computing and storing coefficients for all equations for L^{MT} and r for each muscle before use. Alternatively, continuously differentiable multidimensional cubic splines can be used, but are yet to be examined as a means to estimate musculotendon kinematics. In [113] a single spline function per muscle was used to estimate L^{MT} and r.

2 From EMG Signals to Muscle Activation

This section covers some issues related to the neural controls for a NMS systems and models. In NMS simulation environments, the neural control signal or muscle activation level defines the input of the forward dynamics used to study the human motion. This physiological command indeed specifies the amplitude and the timing of the subject's muscle activation. It can be obtained directly from experimentally measured electromiographic (EMG) signals (EMGs control strategy) or from a synergy analysis (synergies control strategy). Both the control strategies require recording EMG signals from a set of subject's muscles, then a pre-processing of data to obtain a neural control signals utilized in the subsequent steps. EMG pre-processing aims to cut off different non-physiologic signal components due to the acquisition process, such as motion artifacts and 50 Hz noise. It also includes the low pass filtering, to match muscle characteristics, and the optional EMG normalization procedure.

In synergies control strategies, the muscle synergies are first calculated. The main idea behind this method is to express the experimental EMG signals as a weighted sum of a limited number of muscle synergies. This analysis aims to reduce the dimensionality and the redundancy of the human motor system.

Finally, the muscle activation dynamics represent the contribution of the neural control on the activation of each muscle. Once again this processing step is common to both the strategies.

2.1 EMG Pre-Processing

Electromyography is the study of muscle function through the analysis of the electrical signals from the muscles [136]. EMG signals are emitted before muscle contraction and can be detected through superficial non-invasive electrodes. Furthermore, the EMG signal is the result of all the motor unit action potentials occurring during the contraction. This activity, measured at a given electrode location, is expressed by an electric signal (in the order of millivolts) either positive and negative.

EMG signals recording could be affected by unpredictable variables such as: the placement of the electrodes on the subject muscle, the skin characteristics, the amount of tissue between the electrodes and the muscles, the cross talk from nearby muscles, muscle fatigue, the electrodes and amplifier quality and durability through

the acquisition process, the electrical and magnetic noise, etc. The influence of these external factors must be removed, or at least smoothed, before computing the muscle activation [25]. This pre-processing phase can be addressed in different ways.

The first operation is to remove any DC offset and low frequency noise that can be due to the use of low quality amplifiers or electrodes, or due to the movement of the electrodes themselves. This can be done through a high-pass filter with a cutoff frequency in the range of 5–30 Hz, depending on the type of filter and electrodes used. A good strategy is to implement a digital zero-phase delay filter (e.g., forward and backward pass 4th order Butterworth filter). This way filtering does not shift EMG signals in time. The next step is to visually inspect each obtained signal to check the presence of 50 Hz electromagnetic interference. For the affected trials a 50 Hz notch filter (usually of order 10) should be used. Then the signal must be rectified based on its the absolute value for each sample to obtain a *rectified* EMG signal.

2.1.1 EMG Normalization

EMG signals are extremely sensitive to a large number of external factors that can not often be controlled in clinical settings. A very comprehensive review of this problem is available in [38]. EMGs normalization aims to reduce this variability facilitating the comparison of EMG signals across muscles, subjects, or acquisition session from same subject [38, 83]. A concise and precise analysis of the importance of EMG normalization can be found in [83] with a discussion of the dangers of misinterpreting the signals when this step is not preformed correctly.

The general procedure for the EMGs normalization requires to divide the EMG from a specific task by the EMG from a reference contraction or event of the same muscle. Recent papers [28, 32, 33, 38, 77] partially discussed the benefits and limitations of different normalization methods within a more general analysis while a more complete review and critical comparison of normalization strategies can be found in [29]. According to the available results, a standard normalization procedure is still far from being defined.

One of the most used strategies, suggested also by the Journal of Electromyography and Kinesiology (JEK), is the Maximum Voluntary Contraction (MVC) normalization. This strategy divide each EMG signal by the reference one recorded during an MVC task. Similarly, the SENIAM project [96] suggests to use as denominator in the normalization process the EMG from a reference contraction, and uses MVC as an example. Both strategies refer to static MVC although it could also be dynamic. However, non of them provides a guideline to define the best strategy depending on a specific objective. Either JEK and SENIAM advised electromyographers to report information about the joint angles of the subject during the MVC acquisition. The main benefit of using MVC as normalization method is the possibility to understand the level of activation of the muscle during the task in terms of percentage of the MVC. However, electromyographers should pay high attention that subjects are reaching their true maximum contraction during the MVC acquisition, otherwise the results could be uninterpretable.

Another widely used strategy concerns a division by the peak of the EMG recorded during the task or the acquisition. This approach does not need to perform ad-hoc trials. However, most of researches indicate that this method reduces inter–subject variability and has poor intra-subject reliability. Therefore it is better to avoid the use of this strategy to compare EMGs among different trials, muscles or individuals.

2.1.2 Muscle Filtering Effect

The normalized and rectified EMG signals should be low pass filtered to match the muscle filtering effect. Indeed, although the electrical signals that pass through the muscle have components over 100 Hz, the forces that the muscle generates is at much lower frequency. There are many mechanisms in muscle that require this filtering: calcium dynamics, finite amount of time for signals propagation along the muscle, and muscle and tendon viscoelasticity. The cutoff frequency typically used is in the range of 3–10 Hz.

This step is the last one in the pre-processing of the raw EMG signals. The output of this process can be used to directly evaluate muscle activation or elaborated to extrapolate muscle synergies.

2.2 Muscle Synergies

The concept of muscle synergy was proposed for the first time by Bernstein in 1967 [17]. The idea is that the CNS uses this strategy to reduce the redundancy in the motor control task of musculoskeletal system with multiple degrees of freedom. Recent interpretations suggest that afferent signals and supra spinal descending motor control commands interact, select, and correctly activate a low-dimension set of muscle synergies through time modulated activation coefficients. Synergies can be thought as neural networks produced at corticospinal levels, specifying an invariant profile of activation for the motoneurons innervating a set of muscles [31]. The result is a weighted distribution of the neural drives to different muscles. Experimental results, obtained both in humans and animals, support the hypothesis that biomechanical tasks reflect a synergistic muscle control. Moreover, there is evidence that different biomechanical conditions, such as speed and load, share the same synergies [30, 76].

Different studies have used low-dimensional sets of multi-impulse curves within musculoskeletal models of the human lower extremity assessing the mechanical role of muscles during human locomotion [4, 93, 102] and the conceptual idea of muscle synergies in relation to the biomechanics of human and animal movement [58, 79, 94, 123, 137]. Since the multi-muscular EMG patterns observed during motor behaviors have a lower dimensionality with respect to the number of muscles and associated motor units (MTUs) [19, 37], the same excitation patterns can be expressed using a low-dimensional set of muscle synergies. Hence, a low-dimensional controller of single-impulse synergies could be designed to be generic to subjects

and motor tasks, but sufficiently selective to drive a subject-specific musculoskeletal model of the human lower extremity [112]. In this same work, the static behavior and simplified structure of the generic synergies have been compensated using the experimental joint kinematics as an error correction factor. This approach provides a musculoskeletal model of human locomotion which can be operated in an open-loop forward dynamics way without using numerical optimization to match the experimental joint moments, reducing the computational cost. Moreover, since the musculoskeletal is calibrated on a specific subject, it can estimate movement-specific joint moment even if driven by subject-generic and task-generic synergies. In this scenario no EMG recordings are needed for the model operation, allowing its use in the development of neurorehabilitation technologies simplifying the human-robot interface.

A common approach to muscle synergies identification is based on a Non-negative Matrix Factorization (NMF) technique [82]. A good practice when using this technique is pre-process the data with the peak normalization strategy for EMG amplitude (Sec. *EMG Normalization*) where the peak is evaluated across all the available tasks. Then, a normalization in time follows [65, 76]. Finally, a $m \times n$ matrix is created, where m is the number of recorded muscles and n is the number of trial frames per the number of trials per the number of subjects.

The NMF is applied to the matrix with a number of non-negative factors identified together with their associated weightings. The extracted, experimental non-negative factors are linearly combined with their associated weightings to produce an $m \times n$ matrix of reconstructed EMGs and then compared to the original EMG matrix. The NMF is iterated within an optimization procedure adjusting the non-negative factors until they minimize the least squared error between experimental and reconstructed EMG data. In this procedure the dimensionality of the non-negative factor set is increased until the accuracy of the reconstructed EMG data reach a pre-defined threshold. This is assessed by means of the Variation Accounted For (VAF) index, which is defined as:

$$VAF = 1 - SSE/TSS \tag{16}$$

where SSE (sum of squared errors) represents the unexplained variation and TSS (total sum of squares) is the total variation of the EMG data. A minimal VAF value of 80 % is a good choice for the threshold to consider the reconstruction quality as satisfactory [65].

Several other algorithms can be used to identify muscle synergies combination. In [126] these algorithms have been compared on both simulated and experimental data sets with the main goal of investigating their ability to identify the set of synergies from a common data set. The obtained results are quite similar for all the algorithms with no significant differences in performances or accuracy.

2.3 From EMG to Neural Activation

In order to account for the time varying features of the EMG signals, a detailed model of muscle activation dynamics should be considered. In this paragraph, we will refer with the term EMGs (e(t)) both to the pre-processed EMGs and to the synthetic EMG retrieved from the weighting of the muscle synergies.

The next processing steps are indeed common to both the control strategies. The first proposal for modeling the neural activation dynamics was the following first-order linear differential equation [25, 136]:

$$\frac{d\,u(t)}{d(t)} + \left[\frac{1}{\tau_{act}} \cdot (\beta + (1-\beta)e(t))\right] \cdot u(t) \frac{1}{\tau_{act}} e(t) \tag{17}$$

where τ_{act} is the time delay associated to the activation dynamics and β is a constant that can vary in the range $(0, 1)$. This modeling approach captures very well the activation dynamics but requires to be solved numerically for a discrete signal, using a numerical integration approach, such as Runge-Kutta algorithm. Therefore, a more efficient model is required.

A critically damped linear second order differential equation has been used with quite good results [98]. An approximated version of this differential equation have been proposed [25, 110]:

$$u(t) = \alpha e(t-d) - \beta_1 u(t-1) - \beta_2 u(t-2) \tag{18}$$

where d is the electromechanical delay and the coefficients α, β_1 and β_2 define the second order dynamics. The electromechanical delay have been shown to be in a range from 10 to 100 ms [25, 36]. The selection of these four parameter is critical for the stability of the equation. Therefore the following relationships must be verified:

$$\beta_1 = \gamma_1 + \gamma_2 \tag{19}$$

$$\beta_2 = \gamma_1 \times \gamma_2 \tag{20}$$

$$|\gamma_1| < 1 \tag{21}$$

$$|\gamma_2| < 1 \tag{22}$$

Another condition that must be verified ensure the unitary gain of the equation:

$$\alpha - \beta_1 - \beta_2 = 1 \tag{23}$$

Through the combination of previous constrains only the three parameters d, γ_1, and γ_2 are required to fully describe the transformation.

2.4 From Neural Excitation to Muscle Activation

This paragraph illustrates how the nonlinear relation between the neural excitation $u(t)$ and the muscle activation $a(t)$ can be modeled. A possible explanation for this non-linearity can be found in the size principle, i.e. the size of the recruited motor units is related to the force that has to be expressed.

Several studies have shown that the effect of this nonlinearity is significant only at lower excitation (up to 30–40 % of the maximum). For this reason, a first attempt to model this relation, presented in [133], uses a power function in the first 30–40% and a linear function for the remainder. The power function is expressed as:

$$EMG = a \cdot FORCE^{b} \tag{24}$$

where the authors referred with EMG to the neural excitation $u(t)$ and as FORCE to the muscle force (linearly related to the muscle activation $a(t)$).

Both of them indicated in capital letters to underline that are normalized to their maximum value. The coefficients a and b were computed basing on experimental measurements. However, this approach has two main disadvantages: the need to evaluate two parameters and the not-smoothed connection between the two expression.

Another approach correct these disadvantages is proposed in [25, 91]. This solution uses a logarithmic function for the first 30 % and a linear expression for the reminder:

$$\begin{aligned} a(t) &= d\, ln(c\, u(t) + 1) \qquad 0 \leq u(t) \sim 0.3 \\ a(t) &= m\, u(t) + b \qquad\quad \sim 0.3 \leq u(t) < 1 \end{aligned} \tag{25}$$

where the coefficients d, c, m, and b can be simultaneously solved and therefore reduced to a single parameter A, which characterizes the amount of nonlinearity,

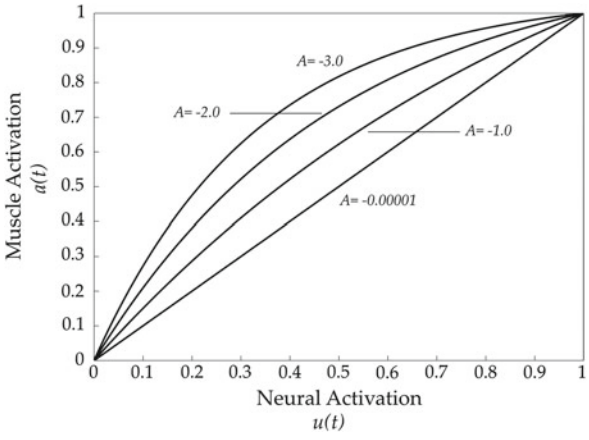

Fig. 5 Changes in the neural excitation u(t) to muscle activation a(t) curve depending on the nonlinear shape factor A

varying from 0 to approximately 0.12. A simpler formulation, [25, 88, 90, 92] is the following:

$$a(t) = \frac{e^{A\,u(t)} - 1}{e^{A} - 1} \tag{26}$$

The coefficient A in Eq. 26 is named nonlinear shape factor and it is allowed to vary from 0 to -3 where $A = -3$ indicates a linear relationship as shown in Fig. 5. The value of A is determined through the usage of the calibration procedure.

3 Differences in Task-Dependent Central Control Strategies for Same or Similar Joint Biomechanics

Neuromuscular control in humans is still unknown due to the high complexity of our neuro-musculoskeletal systems and its high motor redundancy [23, 81, 111]. Humans learn and adapt different dexterous tasks in an interactive manner with external environments taking advantage of their past knowledge of motor actions and their biomechanical structure. [18, 116, 130]. Many elements in the human body dynamically cooperate to perform tasks planned in the brain. Task parameters are planned in different areas in the brain, known as central control unit, to create a motor program that contain the necessary central motor command to perform the task. The central motor commands are then transmitted through the brain stem and spinal cord to alpha-motor neurons which are known are local controllers of the muscular system Fig. 6. Motor neurons in spinal cord drive the muscle contraction to actuate skeletal segments that in turn generate the desire motion and dynamic properties (i.e. forces and torque). Sensory signals are sent to local and central control units during the action execution to modulate the dynamic properties in the biomechanical system.

Scientists suggest that humans centrally control their movements in feed forward system and locally in feedback system [34, 75, 108], also known as open-loop

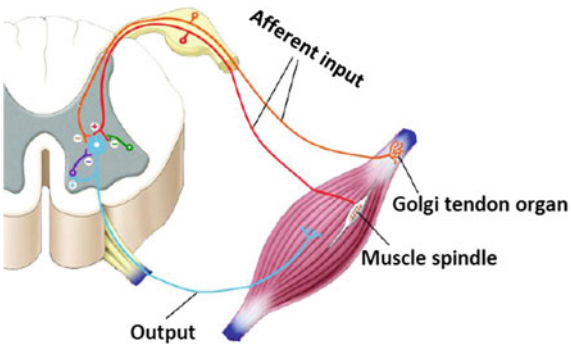

Fig. 6 Basic neural circuit describing the closed-loop control structure of a single muscle

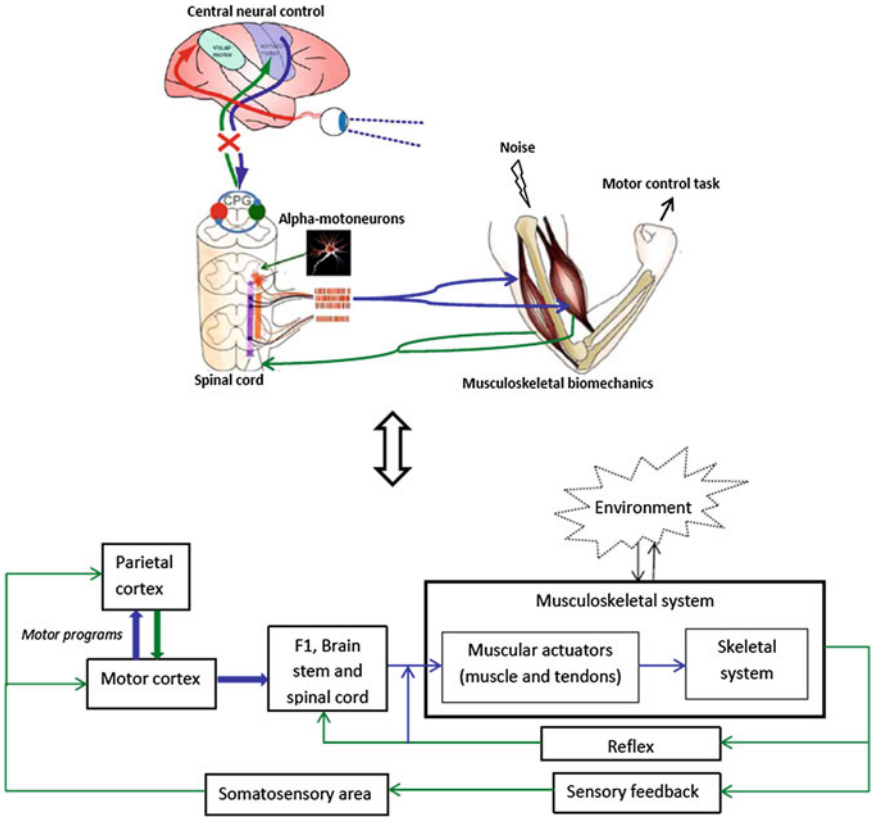

Fig. 7 Basic scheme of neuro-musculoskeletal systems. Blue arrows represent the motor information while green arrows stand for the sensory and feedback information

and closed-loop systems respectively as illustrated in Fig. 7. This basic motor control scheme describes different control levels and sensory information modalities integration in the CNS taking into account the delays caused by the sensory-motor loops that are crucial for some motor actions.

Muscles are the main components in any biomechanical system to generate forces. They are unidirectional force generators and can only contract, therefore they can only pull. Based on that fact, our joints are always actuated by at least two muscles known as agonist and antagonist muscles to bi-directionally control the joint movement like flexion and extension or abduction and adduction in digits. Muscles are activated when a neural signal arrives from an alpha motor neuron through its axons to a target muscle fiber. A large number of muscles can be activated simultaneously to produce a movement and consequently perform a task. Pointing toward an object with the index finger or reaching tasks are typical examples to describe the problem [120]. In robotics, three coordinates of the fingertip in the operational space need to be planned corresponding to three equations, but the number of joints and muscles participating

in such a task is much higher which means that the number of unknown variables (Degrees of freedom) is higher than the number of equations [35]. In consequence, the motor control task can have an infinite number of neural solutions of joint angles and muscle forces. The motor control task could have different neural solutions among different people or even for the same person when solving it several times [69, 81, 109].

Some motor control researchers believe that this motor control redundancy problem is solved at the neural level by our CNS by optimizing (typically minimizing) a cost function (i.e. muscle energy, total muscle force) to select a neural solution [21, 25, 27, 109, 124, 125]. Static and dynamic optimization methods are usually used to describe this hypothesis and estimate the neural solutions. Other researchers, [52, 56, 80, 103, 105], believe that there are no computations of mechanical variables done at the neural level and the CNS cares only about the overall task performance and matching the task requirements beside of the detailed muscle activation characteristics (i.e. recruitment frequency of motor units). An example of this view is the Equilibrium Point hypothesis (EP), originally developed by Feldman in 1960, will be described in more details in this chapter. EP hypothesis is based on the idea of control with thresholds for activation of neuronal pools, it assume that all the mechanical variables (i.e. joint stiffness, muscle and join forces, muscle activity "EMG", etc.) are not directly planned in the CNS, but they emerge when reducing the difference between a referent configuration pre-programmed by the CNS and the actual one.

Muscle redundancy at a joint allows humans to perform isometric or isotonic tasks. A person can produce a constant net joint moment but different muscle activation patterns in static and dynamic tasks [122]. This leads to a variation in co-contraction levels of agonist-antagonist muscles with the net muscle activity with no change on the net joint moment. However, the main contribution of muscle co-contractions in the motor control task is still under-investigation. In this chapter, we presented two neural control frameworks, muscle activation control and equilibrium point control, that account for the muscle co-contraction control and its dependency on the control task.

3.1 Muscle Activation Control

Almost all the motor control hypotheses agree that the CNS controls the muscle contraction locally by alpha motor neurons located in the spinal cord [53, 84, 104] or the brain stem (for facial and neck muscles). Those neurons receive projections of central commands that describe the task parameters (desired spatial pose "position and orientation", velocity, total force... etc.) pre-programmed in the cortical areas of brain and reflex signal for fast movement. Muscle activation control models assume that the CNS pre-compute some unknown variables (i.e. mechanical parameters, muscle activation patterns, ... etc.) based on the task and biomechanical properties and actual state of the neuro-musculoskeletal system [88, 132].

3.1.1 Task-Dependent Muscle Activation Patterns for Static and Dynamic Tasks

Several studies have shown high evidence that the muscle activity patterns are task-dependent [24, 63, 67, 122]. Tax and his colleagues hypothesis suggested that central activation of motor units is different in the control of movement and isometric contractions. They compared the activation behavior of motor units in force task with two conditions of movement task, imposed movements and intended movements. They found that the CNS recruits the motor units during isometric contractions similarly during imposed movement contractions and differently during slow isotonic voluntary movements.

Ghez and his colleagues developed another hypothesis, called pulse-step control, suggesting that the CNS controls movements and isometric contractions by scaling muscle activation patterns. This assumption hypothesize that the projection of task parameters received by alpha-motor neurons is a sequence of a short-lasting pulse and long-lasting step. The hypothesis was then updated by the authors considering the pulse and step commands are separated in the CNS. During isotonic movements (movement task), the pulse amplitude would control the acceleration rate and its duration would define the movement amplitude (e.g. the trajectory of an effector). The step component of the sequence would control the co-contraction level of agonist-antagonist muscle to stop the movement at the final position. During isometric contractions (force task), the pulse amplitude would control the production rate of force and its duration would indirectly define the peak force (e.g. time profile of force). The step part of the command would stop the force production and therefore define the final steady-state force.

Buchanan and his colleagues tested muscle activation patterns in humans when performing two different static tasks, isometric (force control; when joint angles are fixed and joint torque is allowed to vary) and isoinertial (position control; when joint torque is fixed and joint angles are allowed to vary) tasks. In their study, they aimed to see if there is a difference in muscle activation patterns (e.g. muscle synergies) even though the joint angles and torques are identical. Their hypothesis suggests that the difference in synergic activations occur not only between static isometric and dynamic isotonic tasks but also between static isometric and isoinertial tasks. This switch in the central control strategy depends on the control task (i.e. force control for isometric tasks or position control for isoinertial tasks).

3.1.2 Muscle Co-Activation Patterns

As we showed in the previous paragraph, muscle co-contraction patterns vary not only with the length and force but also with the load characteristics (e.g. isometric, isotonic or elastic load) on the joint or its stability condition [39, 68].

De Serres and his colleagues have found a little effect of a stable load (constant or elastic) and a big effect of unstable load on the co-contraction of wrist flexor and extensor muscles. The muscle co-contraction was dramatically greater for the

unstable load than the stable load. They also tested the effect of muscle co-contraction on the stretch reflex response and found a major effect for a stable load than for an unstable load. In consequence, the joint stiffness was more dramatically affected for a stable load than an unstable load. They concluded that the muscle co-activation patterns (e.g. muscle synergies) of the central control, and therefore the muscle co-contraction, are different depending on the load stability condition. They found no evidence of a significant contribution of phasic stretch reflexes in the joint stiffness although their results showed that magnitude of reflex response increases with the co-contraction level. Hence, they concluded that the stretch reflex modulation is independent from the tonic muscle activation control and dependent on the load stability.

Heiden and her colleagues explored the co-contraction patterns in Knee Osteoarthritis (OA) patients. They have shown that the level of muscle activation varies with the loading and the reduction of pain and adduction moments. Their study stated that the levels of net muscle activation increased during loading and early stance to possibly alter the stabilization and articular loading of knee joint. They found a significant difference in muscle activation strategies between OA patients and healthy subjects. OA patients utilize a directed co-contraction strategy to exhibit greater lateral muscle activation during loading, early stance and mid-stance while heathy subjects utilize it to predominantly exhibit medial muscle activation during the same tasks. Some studies showed that the increment of the co-contraction level does not increase the net moment (net moment = constant) but the net muscle activity [89]. They also observed that OA patients increase the level of net muscle activity and laterally directed co-contraction even as the same joint moment and posture while heathy subjects utilizes lower co-contraction levels. This result suggest that OA patients use this mechanism to reduce the pain resulted from external knee adduction moments. It is also worth noting that no difference in co-contraction level or net muscle activity was observed between control and stroke groups in late stance.

3.2 Threshold Position Control

As we mentioned above, a second view on neural control of muscles, called threshold (referent) position control or equilibrium point control, contrasts the muscle activation control hypotheses. It does not consider any particular computation of the unknown system variables at the neural level, but an emergence of those variables when the neuro-musculoskeletal system attempts to attain a referent configuration of an effector [53–55]. In other words, neither trajectories (i.e. trajectory of an effector, force/torque profiles, joint stiffness, etc.) nor motor commands (muscle activity "EMG patterns") are directly specified by neural control levels but only a referent configuration and those mechanical variables emerge when reducing the difference between a referent configuration pre-programmed by the CNS with the actual one. This automatic mechanism occurs in alpha-motoneurons which reduces the error between a central input (referent control signal) and afferent input (feedback signals,

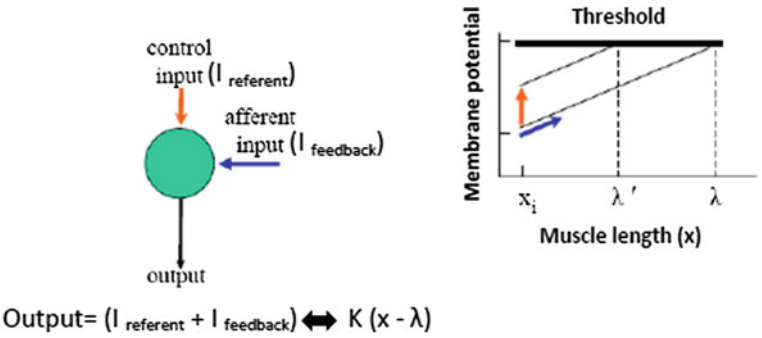

Fig. 8 Alpha-motoneuron is represented as a servo controller in the left-hand image. Regulation of threshold muscle length in neurons is shown in the right hand image. The neuron works as a servo controller to reduce the error between the actual muscle length and the control variable (lambda) to obtain a referent configuration of the body segment pre-programmed in the brain. parameter is projected from task parameters though muscle synergy mapping. It can be shifted by the CNS to define a new referent configuration

i.e. muscle spindle feedback), as illustrated in Fig. 8 (motoneurons). The central input is a projection of high level commands that describe a referent configuration. The afferent feedback provides the CNS information about deviation of the actual (emergent) position of an effector from their referent position specified by the brain. The neuron can generate action potentials when the neural membrane potential due to the input excitatory sources reaches a threshold according to all-or-non law. The neuron output changes the state of an effector. The frequency of action potentials generated by the neuron depends on all afferent excitatory signals.

Equilibrium Point hypothesis assumes that the CNS controls the muscle activation with thresholds for activation of neuronal pools, this neural control strategy is called threshold position control.

Threshold position is a parameter that pre-determines where, in spatial coordinates, muscles can work without pre-determining how they should work in terms of EMG patterns, forces and kinematics. The referent signal is normally lower the membrane threshold in healthy subjects otherwise the neuron will be always active generating action potentials at the highest possible frequency independently of the afferent feedback input. This is because the neuronal membrane potential is over the threshold. Hence, the membrane potential should depend on both referent control and feedback inputs. Based on threshold control hypothesis, the CNS regulates the membrane potential through the referent position control level as illustrated in Fig. 8. It is clear from the figure that a low level and a high level of referent control signal will lead to two different referent configurations (e.g. two different muscle lengths and forces). If the referent control level is constant, the neural membrane potential to reach the threshold will depend on the feedback source. If the referent control level is shifted to a higher level, the membrane potential will be closer to reach the threshold, and therefore the neuron will need less feedback excitation to fire action

potentials. This mechanism will produce two different muscle lengths leading to two different configurations of the body segments or/and force production.

EP hypothesis suggests that the central control defines the set of R and C commands at the joint level which delivers information about the referent configuration intentionally planned (e.g.Θ). R command and C command are addressed as reciprocal and co-activation [52, 85]. These commands are then projected at the corticospinal level to provide control variable (λ) at the muscle level addressed as the threshold of tonic stretch reflex. This means that each muscle can have its own λ according to its fiber length and biomechanical properties and connections, but the same R and C command set corresponding to a referent configuration (e.g. joint angles Θ).

The transition previously described corresponds to a shift in the characteristic of muscle force-length. For agonist-antagonist muscle actuation, R-command leads to a unidirectional shift of the two muscle characteristics (R = sum (λ_1, λ_2)) while C-command leads to an opposite directional shift of the two muscle characteristics (C = diff (λ_1, λ_2)). Changes in R and C commands reflect a change joint movement and joint stiffness respectively. Based on EP hypothesis, it may happen voluntarily following a change in the central commands (R and/or C commands) which lead to a change in the threshold level of the tonic stretch reflex (λ) or involuntarily (R and C commands are constant, λ is constant) following a change in the external load as illustrated in Fig. 9.

EP hypothesis suggests that co-contractions of agonist-antagonist muscles are modulated through C-commands. Changes in this command reflect a variation in the joint stiffness and damping when the musculoskeletal system is deviated from its equilibrium states [52]. C-command can be modulated independently of R-command during static or dynamics task [85]. This result would suggest a multi-contribution of C-command in joint stability and movement speed.

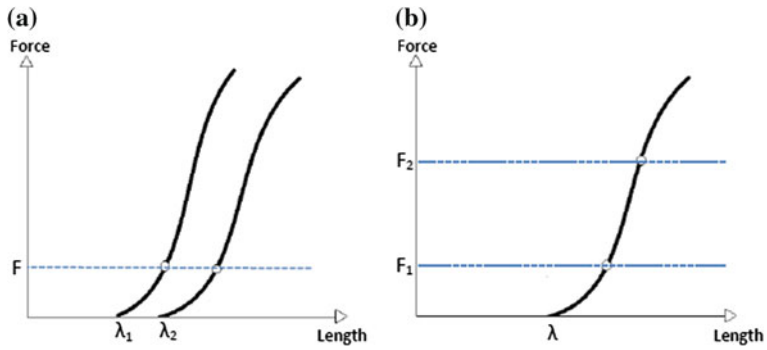

Fig. 9 **a** voluntarily movement produced by a shift in the threshold level of the tonic stretch reflex (λ) through a change in the central commands (R and/or C commands) **b** involuntarily movement produced by a change in the external load at constant intentional neural control (R and C commands are constant, λ is constant)

4 Personalized Musculoskeletal Modeling

Computational musculoskeletal models can provide an accurate knowledge of the physiological loading conditions on the skeletal system during human movements and allow quantifying factors (e.g. muscle moment arms, joint motions) that affect musculoskeletal function, Thus, it may significantly improve clinical treatments in several orthopedics and neurological contexts [10, 11, 15, 44]. Musculoskeletal models have been used to study stroke [5], spinal cord injury [9], bone fractures, joint osteoarthritis [64], orthopedic surgical procedures such as Arthroplasty and neurological disease such as cerebral palsy [42].

Muscle and joint contact forces during motion are currently not measurable in vivo with non-invasive devices. Computational modeling of the musculoskeletal system is the only practicable method that can provide an approach to analyze loading of muscle and joint. Computer and information technologies have recentrly advanced computational modeling to deal with important challenges in clinical biomechanics. The development of new modeling methods and numerical simulation algorithms, which are computationally efficient, are increasingly raising the interest in musculoskeletal modeling and simulation among the biomechanical and medical communities.

Every patient is different and possesses unique anatomical, neurological, and functional characteristics that may significantly affect optimal treatment of the patient. Personalized computational models of the NMS system can facilitate prediction of patient-specific functional outcome for different treatment designs and provide useful information for clinicians. Personalized models may reduce the likelihood that different clinicians will plan different treatments given the same patient data [58]. Depending on the intended clinical application, a personalized NMS model might account for patient specific anatomical (e.g., skeletal structure and muscle lines of action), physiological (e.g., muscle force-generating properties), and/or neurological (e.g., constraints on achievable muscle excitation patterns) characteristics, all within the context of a multibody dynamic model [58].

Personalized computational models can be derived by generic models or subject-specific models with different levels of subject-specific details.

4.1 Generic Models

The existing musculoskeletal models in use have some limitations. Several studies have used generic musculoskeletal models derived from average adult anatomy [51, 106]. In addition, many software packages for biomechanical analysis of muscle function are based on biomechanical studies of cadaveric specimens, and use the musculoskeletal geometry of a healthy, average-sized adult male with normal musculoskeletal geometry [9, 43, 44]. These generic models apply variations in subject size by scaling [46, 57, 87], based on three-dimensional positions of markers placed on selected anatomical landmarks and measured during a static, standing trial.

The lower-limb Delp model [44, 45] has been widely adopted for a variety of biomechanical investigations. This generic model is based on several experimental studies, and has been altered and refined to different purposes [6, 101]. But dataset inconsistency and limitation of in vivo measurements make some difficulties in the identification of model parameters. And the use of generic models in representation of a wide population may not be robust.

Two critical tasks in process of using personalized models are Calibration and Validation [58]. Since generic models are constructed from detailed anatomic measurements performed on cadaver specimens, a model personalization/calibration process is needed. Four proposed model calibration steps that should be performed in whole or in part to transform a generic model into a personalized model include geometric calibration, kinematic calibration, kinetic calibration and neurologic calibration. Validation of clinical predictions is the other major challenge faced by personalized models will ultimately require randomized controlled trials, where outcomes are compared between patients whose treatments were planned with a personalized model and those whose treatments were not [58].

In fact personalized models have the greatest potential to impact clinic practice, but generic models can still provide significant clinical benefits. Generic models were used to simulate bone deformities [10], risk of bone fracture [128], and tendon transfer surgeries [46]. However, a recent study has proved that such models provide inaccurate analysis of muscle function even for a healthy adult male [115].

A growing concern is being raised about the accuracy of scaled-generic models, since the musculoskeletal system is very intricate and large anatomical variations exist among individuals, scaled-generic models may not be able to fit to all variability of musculoskeletal geometry and tissue properties among individuals. This is particularly when the case of study is a pathological musculoskeletal condition. A recent study has proved that such models provide inaccurate analysis of muscle function even for a healthy adult male, this studies showed significant differences in muscle moment arm lengths, musculotendon lengths and gait kinematics calculated with subject-specific models created from MRI and scaled-generic models [114]. The musculoskeletal geometry determines moment arm and thereby the moment about a joint produced by a given musculotendon force. A study showed how variability of muscle attachments affects muscle moment arms (MALs) [48]. Also the effects of bone geometry on the moment-generating capacity of the muscles has been shown [45]. Thus, the different musculoskeletal geometry due to size or pathology can also affect the accuracy of results derived from generic models.

Since the results of simulations are often sensitive to the accuracy of the functional musculoskeletal model, individualized musculoskeletal models may be a better alternative.

4.2 Subject-Specific Models

Despite the growing concern on the use of scaled-generic model to investigate skeletal load, A few studies performed using different levels of subject-specific details [58, 127]. Few attempts have been made to create subject-specific models for skeletal load predictions, and it not clarified to which extent it is important to obtain different subject-specific parameters. Personalization process involve tissue geometries reconstructions, calculation of tissue inertial properties, definition of location and orientation of joint axes from anatomical landmarks, definition of musculotendon architecture. In addition to importance of validation problem of model predictions, it is difficult to collect all necessary data in the research and clinical practice. Another problem is the lack of valuable methods and frameworks to create subject-specific models and simulations. Developing these kind of methods requiring extensive effort with skilled expertise and time. The musculoskeletal geometry for a specific subject can be extracted from MRI or CT-scan images with a good accuracy and low level of invasiveness and it can be used to study in vivo the complex geometric relationships among the muscles, bones, and other structures. The level of subject-specific detail also involves additional measurements, e.g., body motion, ground reaction forces, muscle activity, which can be obtained through technologies for human movement analysis such as stereophotogrammetry, 3D fluoroscopy, EMG, force platforms.

As it is mentioned, one problem is about lack of valuable methods and frameworks available. The other problem is about availability of required data, collecting these data are dependent on mentioned technologies and cannot be always collected in the research and clinical practice and this arises time- and cost-related problems.

Important research has been performed to incorporate more accurate MR-based models of musculotendon geometry into multibody musculoskeletal models [12, 15, 20], however it is time-consuming and requires extensive imaging protocols to capture the muscle and joint geometry at different limb positions. Subject-specific musculoskeletal modelling also addresses the problem of image segmentation, which consists of extracting anatomical structures from medical image data such as MRI. Semiautomatic or fully automatic segmentation methods are fast but inaccurate since muscle distinction is often difficult or impossible to assess with currently used methods. Thus, muscles volumetric representations are most often and most accurately acquired by defining muscle contours manually.

4.3 Software for Personalized Musculoskeletal Modeling

Personalized musculoskeletal modeling and biomechanical load analyzing are increasingly performed by using commercial, freeware and in-house custom-built software. And also several generic models are available for the biomechanical community. As an example, OpenSim is a freely available musculoskeletal modeling and simulation application and libraries specialized for modeling, simulating,

and analyzing the neuromusculoskeletal system [41]. OpenSim provides musculoskeletal modeling elements such as biomechanical joints, muscle actuators, ligament forces, compliant contact, and controllers; and tools for fitting generic models to subject-specific data, performing inverse kinematics and forward dynamic simulations. It performs an array of physics-based analyses to delve into the behavior of musculoskeletal models by employing multibody system dynamics codes. Models are publicly available and are often reused for multiple investigations because they provide a rich set of behaviors that enables different lines of inquiry (Fig. 10) [41, 119].

It is also possible to add subject-specific information to biomechanical models using these modeling and simulation environments. However the software users and developers have to necessarily set up specific modeling frameworks that involve an important pre-processing phase to create the models. Depending on the level of subject specific details, this process needs a skilled expertise to process imaging data, define the features of the multibody systems, create models and simulation setups in the appropriate file formats, and particularly develop codes to create efficient modeling frameworks.

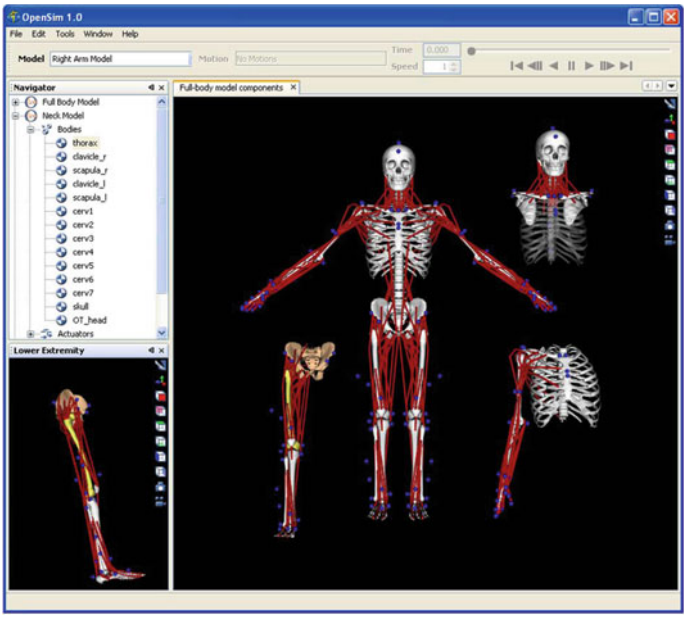

Fig. 10 Screenshot from OpenSim. Models of different musculoskeletal structures, including the lower extremity, upper extremity, and neck, can be loaded, viewed and analyzed [41]

References

1. Amazon.it: Theory and Application of Digital Signal Processing—Libri. http://www.amazon.it/Theory-Application-Digital-Signal-Processing/dp/0139141014
2. Ackermann, M., van den Bogert, A.J.: Optimality principles for model-based prediction of human gait. J. Biomech. **43**(6), 1055–60 (2010). doi:10.1016/j.jbiomech.2009.12.012. http://www.pubmedcentral.nih.gov/articlerender.fcgi?artid=2849893&tool=pmcentrez&rendertype=abstract
3. Ackermann, M., van den Bogert, A.J.: Predictive simulation of gait in rehabilitation. In: Annual International Conference of the IEEE Engineering in Medicine and Biology Society, pp. 5444–7. (2010). doi:10.1109/IEMBS.2010.5626512. http://www.ncbi.nlm.nih.gov/pubmed/21096280
4. Allen, J., Neptune, R.: Three-dimensional modular control of human walking. J. Biomech. **45**(12), 2157–2163 (2012)
5. Allen, P.E., Jenkinson, A., Stephens, M.M., O'Brien, T.: Abnormalities in the uninvolved lower limb in children with spastic hemiplegia: the effect of actual and functional leg-length discrepancy. J. Pediatr. Orthop. **20**(1), 88–92. http://www.ncbi.nlm.nih.gov/pubmed/10641696
6. Anderson, F.C., Pandy, M.G.: A Dynamic optimization solution for vertical jumping in three dimensions. Comput. Methods Biomech. Biomed. Eng. **2**(3), 201–231 (1999). doi:10.1080/10255849908907988. http://www.ncbi.nlm.nih.gov/pubmed/11264828
7. Anderson, F.C., Pandy, M.G.: Dynamic optimization of human walking. J. Biomech. Eng. **123**(5), 381–90 (2001). http://www.ncbi.nlm.nih.gov/pubmed/11601721
8. Anderson, F.C., Pandy, M.G.: Static and dynamic optimization solutions for gait are practically equivalent. J. Biomech. **34**(2), 153–161 (2001)
9. Arnold, A.S., Anderson, F.C., Pandy, M.G., Delp, S.L.: Muscular contributions to hip and knee extension during the single limb stance phase of normal gait: a framework for investigating the causes of crouch gait. J. Biomech. **38**(11), 2181–9 (2005). doi:10.1016/j.jbiomech.2004.09.036. http://www.ncbi.nlm.nih.gov/pubmed/16154404
10. Arnold, A.S., Delp, S.L.: Rotational moment arms of the medial hamstrings and adductors vary with femoral geometry and limb position: implications for the treatment of internally rotated gait. J. Biomech. **34**(4), 437–47 (2001). http://www.ncbi.nlm.nih.gov/pubmed/11266666
11. Arnold, A.S., Liu, M.Q., Schwartz, M.H., Ounpuu, S., Dias, L.S., Delp, S.L.: Do the hamstrings operate at increased muscle-tendon lengths and velocities after surgical lengthening? J. Biomech. **39**(8), 1498–506 (2006). doi:10.1016/j.jbiomech.2005.03.026. http://www.ncbi.nlm.nih.gov/pubmed/15923009
12. Arnold, A.S., Salinas, S., Asakawa, D.J., Delp, S.L.: Accuracy of muscle moment arms estimated from MRI-based musculoskeletal models of the lower extremity. Computer aided surgery : official. J. Int. Soc. Comput. Aided Surg. **5**(2), 108–19 (2000). doi: 10.1002/1097-0150(2000)5:2⟨108::AID-IGS5⟩3.0.CO;2-2. http://www.ncbi.nlm.nih.gov/pubmed/10862133
13. Arnold, E.M., Delp, S.L.: Fibre operating lengths of human lower limb muscles during walking. Philos. Trans. R. Soc. Lond. Ser. B Biol. Sci. **366**(1570), 1530–9 (2011). doi:10.1098/rstb.2010.0345. http://www.pubmedcentral.nih.gov/articlerender.fcgi?artid=3130447&tool=pmcentrez&rendertype=abstract
14. Arnold, E.M., Ward, S.R., Lieber, R.L., Delp, S.L.: A model of the lower limb for analysis of human movement. Ann. Biomed. Eng. **38**(2), 269–79 (2010). doi:10.1007/s10439-009-9852-5. http://www.pubmedcentral.nih.gov/articlerender.fcgi?artid=2903973&tool=pmcentrez&rendertype=abstract
15. Asakawa, D.S., Blemker, S.S., Rab, G.T., Bagley, A., Delp, S.L.: Three-dimensional muscle-tendon geometry after rectus femoris tendon transfer. J. Bone Jt. Surg. (American Volume) **86-A**(2), 348–54 (2004). http://www.ncbi.nlm.nih.gov/pubmed/14960681
16. Audu, M.L., Davy, D.T.: The influence of muscle model complexity in musculoskeletal motion modeling. J. Biomech. Eng. **107**(2), 147–57 (1985). http://www.ncbi.nlm.nih.gov/pubmed/3999711

17. Bernstein, N.A.: The Co-ordination and reRgulation of Movements. Pergamon Press, Oxford (1967)
18. Bernstein, N.A.: On dexterity and its development. In: Latash, M.L., Turvey, M.T. (eds.) On Dexterity and its Development, pp. 3–246. Lawrence Erlbaum Associates, New Jersey (1996)
19. Bizzi, E., Cheung, V.C.K., D'Avella, A., Saltiel, P., Tresch, M.: Combining modules for movement. Brain Res. Rev. **57**(1), 125–33 (2008). doi:10.1016/j.brainresrev.2007.08.004. http://www.ncbi.nlm.nih.gov/pubmed/18029291
20. Blemker, S.S., Asakawa, D.S., Gold, G.E., Delp, S.L.: Image-based musculoskeletal modeling: applications, advances, and future opportunities. J. Magn. Reson. Imaging (JMRI) **25**(2), 441–51 (2007). doi:10.1002/jmri.20805. http://www.ncbi.nlm.nih.gov/pubmed/17260405
21. Bottasso, C.L., Prilutsky, B.I., Croce, A., Imberti, E., Sartirana, S.: A numerical procedure for inferring from experimental data the optimization cost functions using a multibody model of the neuro-musculoskeletal system. Multibody Syst. Dyn. **16**(2), 123–154 (2006). doi:10.1007/s11044-006-9019-1. http://link.springer.com/10.1007/s11044-006-9019-1
22. Brand, P.W., Beach, R.B., Thompson, D.E.: Relative tension and potential excursion of muscles in the forearm and hand. J. Hand Surg. **6**(3), 209–19 (1981). http://www.ncbi.nlm.nih.gov/pubmed/7240676
23. Buchanan, T.S., Kim, A.W., Lloyd, D.G.: Selective muscle activation following rapid varus/valgus perturbations at the knee. Med. Sci. Sports Exerc. **28**(7), 870–6 (1996). http://www.ncbi.nlm.nih.gov/pubmed/8832541
24. Buchanan, T.S., Lloyd, D.G.: Muscle activity is different for humans performing static tasks which require force control and position control. Neurosci. Lett. **194**(1–2), 61–64 (1995)
25. Buchanan, T.S., Lloyd, D.G.: Neuromusculoskeletal modeling: estimation of muscle forces and joint moments and movements from measurements of neural command. J. Appl. . . . **20**(4), 367–395 (2004). http://www.ncbi.nlm.nih.gov/pmc/articles/PMC1357215/
26. Buchanan, T.S., Lloyd, D.G., Manal, K., Besier, T.F.: Neuromusculoskeletal modeling: estimation of muscle forces and joint moments and movements from measurements of neural command. J. Appl. Biomech. **20**(4), 367–95 (2004). http://www.pubmedcentral.nih.gov/articlerender.fcgi?artid=1357215&tool=pmcentrez&rendertype=abstract
27. Buchanan, T.S., Lloyd, D.G., Manal, K., Besier, T.F.: Estimation of muscle forces and joint moments using a forward-inverse dynamics model. Med. Sci. Sports Exerc. **37**(11), 1911–6 (2005). http://www.ncbi.nlm.nih.gov/pubmed/16286861
28. Burden, A.: Surface electromyography. Biomech. Eval. Mov. Sport Exerc. 77 (2007)
29. Burden, A.: How should we normalize electromyograms obtained from healthy participants? What we have learned from over 25 years of research. J. Electromyogr. Kinesiol. **20**(6), 1023–35 (2010). doi:10.1016/j.jelekin.2010.07.004. http://www.ncbi.nlm.nih.gov/pubmed/20702112
30. Cappellini, G., Ivanenko, Y.P., Poppele, R.E., Lacquaniti, F.: Motor patterns in human walking and running. J. Neurophysiol. **95**(6), 3426–37 (2006). doi:10.1152/jn.00081.2006. http://jn.physiology.org/content/95/6/3426
31. Cheung, V.C.K., Piron, L., Agostini, M., Silvoni, S., Turolla, A., Bizzi, E.: Stability of muscle synergies for voluntary actions after cortical stroke in humans. Proc. Natl. Acad. Sci. USA **106**(46), 19,563–8 (2009). doi:10.1073/pnas.0910114106. http://www.pubmedcentral.nih.gov/articlerender.fcgi?artid=2780765&tool=pmcentrez&rendertype=abstract
32. Clarys, J.P.: Electromyography in sports and occupational settings: an update of its limits and possibilities. Ergonomics **43**(10), 1750–62 (2000). doi:10.1080/001401300750004159. http://www.ncbi.nlm.nih.gov/pubmed/11083153
33. Clarys, J.P., Cabri, J.: Electromyography and the study of sports movements: a review. J. Sports Sci. **11**(5), 379–448 (1993). doi:10.1080/02640419308730010. http://www.ncbi.nlm.nih.gov/pubmed/8301704
34. Collins, J.J., De Luca, C.J.: Open-loop and closed-loop control of posture: a random-walk analysis of center-of-pressure trajectories. Exp. Brain Res. Exp. Hirnforsch. Exp. Cereb. **95**(2), 308–318 (1993)

35. Conkur, E.S., Buckingham, R.: Clarifying the definition of redundancy as used in robotics (1997)
36. Corcos, D.M., Gottlieb, G.L., Latash, M.L., Almeida, G.L., Agarwal, G.C.: Electromechanical delay: an experimental artifact. J. Electromyogr. Kinesiol. Off. J. Int. Soc. Electrophysiol. Kinesiol. **2**(2), 59–68 (1992). doi:10.1016/1050-6411(92)90017-D. http://www.ncbi.nlm.nih.gov/pubmed/20719599
37. D'Avella, A., Saltiel, P., Bizzi, E.: Combinations of muscle synergies in the construction of a natural motor behavior. Nat. Neurosci. **6**(3), 300–8 (2003). doi:10.1038/nn1010. http://www.ncbi.nlm.nih.gov/pubmed/12563264
38. De Luca, C.: The use of surface electromyography in biomechanics. J. Appl. Biomech. **13**(2), 135–163 (1997)
39. De-Serres, S.J., Milner, T.: Wrist muscle activation patterns and stiffness associated with stable and unstable mechanical loads. Exp. Brain Res. 451–458 (1991). http://link.springer.com/article/10.1007/BF00228972
40. Delp, S.L.: Surgery simulation: a computer graphics system to analyze and design musculoskeletal reconstructions of the lower limb (1990). http://books.google.it/books/about/Surgery_Simulation.html?id=ipzVPAAACAAJ&pgis=1
41. Delp, S.L., Anderson, F.C., Arnold, A.S., Loan, P., Habib, A., John, C.T., Guendelman, E., Thelen, D.G.: OpenSim: open-source software to create and analyze dynamic simulations of movement. IEEE Trans. Bio-med. Eng. **54**(11), 1940–50 (2007). doi:10.1109/TBME.2007.901024. http://www.ncbi.nlm.nih.gov/pubmed/18018689
42. Delp, S.L., Arnold, A.S., Speers, R.A., Moore, C.A.: Hamstrings and psoas lengths during normal and crouch gait: implications for muscle-tendon surgery. J. Orthop. Res. Off. Publ. Orthop. Res. Soc. **14**(1), 144–51 (1996). doi:10.1002/jor.1100140123. http://www.ncbi.nlm.nih.gov/pubmed/8618157
43. Delp, S.L., Loan, J.P.: A graphics-based software system to develop and analyze models of musculoskeletal structures. Comput. Biol. Med. **25**(1), 21–34 (1995). http://www.ncbi.nlm.nih.gov/pubmed/7600758
44. Delp, S.L., Loan, J.P., Hoy, M.G., Zajac, F.E., Topp, E.L., Rosen, J.M.: An interactive graphics-based model of the lower extremity to study orthopaedic surgical procedures. IEEE Trans. Bio-med. Eng. **37**(8), 757–67 (1990). doi:10.1109/10.102791. http://www.ncbi.nlm.nih.gov/pubmed/2210784
45. Delp, S.L., Maloney, W.: Effects of hip center location on the moment-generating capacity of the muscles. J. Biomech. **26**(4), 485–499 (1993)
46. Delp, S.L., Ringwelski, D.A., Carroll, N.C.: Transfer of the rectus femoris: effects of transfer site on moment arms about the knee and hip. J. Biomech. **27**(10), 1201–11 (1994). http://www.ncbi.nlm.nih.gov/pubmed/7962008
47. Diedrichsen, J., Shadmehr, R., Ivry, R.B.: The coordination of movement: optimal feedback control and beyond. Trends Cogn. Sci. **14**(1), 31–9 (2010). doi:10.1016/j.tics.2009.11.004. http://www.ncbi.nlm.nih.gov/pubmed/20005767
48. Duda, G.N., Brand, D., Freitag, S., Lierse, W., Schneider, E.: Variability of femoral muscle attachments. J. Biomech. **29**(9), 1185–90 (1996). http://www.ncbi.nlm.nih.gov/pubmed/8872275
49. Eisenberg, E., Hill, T.L., Chen, Y.: Cross-bridge model of muscle contraction. Quantitative analysis. Biophys. J. **29**(2), 195–227 (1980). doi:10.1016/S0006-3495(80)85126–5. http://www.pubmedcentral.nih.gov/articlerender.fcgi?artid=1328691&tool=pmcentrez&rendertype=abstract
50. Epstein, M., Herzog, W.: Theoretical models of skeletal muscle: biological and mathematical considerations (1998). http://www.amazon.com/Theoretical-Models-Skeletal-Muscle-Considerations/dp/0471969559
51. Erdemir, A., McLean, S., Herzog, W., van den Bogert, A.J.: Model-based estimation of muscle forces exerted during movements. Clin. Biomech. (Bristol, Avon) **22**(2), 131–54 (2007). doi:10.1016/j.clinbiomech.2006.09.005. http://www.ncbi.nlm.nih.gov/pubmed/17070969

52. Feldman, A.G.: Superposition of motor programs-II. Rapid forearm flexion in man. Neuroscience **5**(1), 91–5 (1980). http://www.ncbi.nlm.nih.gov/pubmed/7366846
53. Feldman, A.G.: Once more on the equilibrium-point hypothesis (lambda model) for motor control. J. Mot. Behav. **18**(1), 17–54 (1986). http://www.ncbi.nlm.nih.gov/pubmed/15136283
54. Feldman, A.G., Goussev, V., Sangole, A., Levin, M.F.: Threshold position control and the principle of minimal interaction in motor actions. Prog. Brain Res. **165**, 267–81 (2007). doi:10.1016/S0079-6123(06), 65017–6. http://www.ncbi.nlm.nih.gov/pubmed/17925252
55. Feldman, A.G., Latash, M.L.: Testing hypotheses and the advancement of science: recent attempts to falsify the equilibrium point hypothesis. Exp. Brain Res. **161**(1), 91–103 (2005). doi:10.1007/s00221-004-2049-0. http://www.ncbi.nlm.nih.gov/pubmed/15490137
56. Feldman, A.G., Levin, M.F.: The equilibrium-point hypothesis-past, present and future. Adv. Exp. Med. Biol. **629**, 699–726 (2009). doi:10.1007/978-0-387-77064-2_38. http://www.ncbi.nlm.nih.gov/pubmed/19227529
57. Fox, M.D., Reinbolt, J.A., Ounpuu, S., Delp, S.L.: Mechanisms of improved knee flexion after rectus femoris transfer surgery. J. Biomech. **42**(5), 614–9 (2009). doi:10.1016/j.jbiomech.2008.12.007. http://www.pubmedcentral.nih.gov/articlerender.fcgi?artid=2929172&tool=pmcentrez&rendertype=abstract
58. Fregly, B.J., Boninger, M.L., Reinkensmeyer, D.J.: Personalized neuromusculoskeletal modeling to improve treatment of mobility impairments: a perspective from European research sites. J. Neuroeng. Rehabil. **9**(1), 18 (2012). doi:10.1186/1743-0003-9-18. http://www.jneuroengrehab.com/content/9/1/18
59. G. Feldman, A., F. Levin, M., Mitnitski, A.M.: 1998 ISEK Congress Keynote Lecture. J. Electromyogr. Kinesiol. **8**(6), 383–390 (1998). doi:10.1016/S1050-6411(98)00019–4. http://www.sciencedirect.com/science/article/pii/S1050641198000194
60. Gabriel, D., Kamen, G.: Essentials of electromyography. http://www.humankinetics.com/products/all-products/essentials-of-electromyography-ebook
61. Garner, B.A., Pandy, M.G.: The obstacle-set method for representing muscle paths in musculoskeletal models. Comput. Methods Biomech. Biomed. Eng. **3**(1), 1–30 (2000). doi:10.1080/10255840008915251. http://www.ncbi.nlm.nih.gov/pubmed/11264836
62. Garner, B.A., Pandy, M.G.: Estimation of musculotendon properties in the human upper limb. Ann. Biomed. Eng. **31**(2), 207–20 (2003). http://www.ncbi.nlm.nih.gov/pubmed/12627828
63. Ghez, C., Gordon, J.: Trajectory control in targeted force impulses. Exp. Brain Res. **67**(2) (1987). doi:10.1007/BF00248545. http://link.springer.com/10.1007/BF00248545
64. Gill, H.S., O'Connor, J.J.: Heelstrike and the pathomechanics of osteoarthrosis: a simulation study. J. Biomech. **36**(11), 1617–24 (2003). http://www.ncbi.nlm.nih.gov/pubmed/14522202
65. Gizzi, L., Nielsen, J.r.F.k., Felici, F., Ivanenko, Y.P., Farina, D.: Impulses of activation but not motor modules are preserved in the locomotion of subacute stroke patients. J. Neurophysiol. **106**(1), 202–10 (2011). doi:10.1152/jn.00727.2010. http://www.ncbi.nlm.nih.gov/pubmed/21511705
66. Gordon, A.M., Huxley, A.F., Julian, F.J.: The variation in isometric tension with sarcomere length in vertebrate muscle fibres. J. Physiol. **184**(1), 170–92 (1966). http://www.pubmedcentral.nih.gov/articlerender.fcgi?artid=1357553&tool=pmcentrez&rendertype=abstract
67. Gottlieb, G.L., Corcos, D.M., Agarwal, G.C.: Strategies for the control of voluntary movements with one mechanical degree of freedom. Behav. Brain Sci. **12**(02), 189–210 (1989). http://journals.cambridge.org/abstract_S0140525X00048238
68. Gribble, P.L., Ostry, D.J.: Compensation for loads during arm movements using equilibrium-point control. Exp. Brain Res. **135**(4), 474–82 (2000). http://www.ncbi.nlm.nih.gov/pubmed/11156311
69. Guigon, E., Baraduc, P., Desmurget, M.: Computational motor control: redundancy and invariance. J. Neurophysiol. **97**(1), 331–47 (2007). doi:10.1152/jn.00290.2006. http://jn.physiology.org/content/97/1/331
70. Guimaraes, A.C., Herzog, W., Hulliger, M., Zhang, Y.T., Day, S.: Effects of muscle length on the EMG-force relationship of the cat soleus muscle studied using non-periodic stimulation of

ventral root filaments. J. Exp. Biol. **193**, 49–64 (1994). http://www.ncbi.nlm.nih.gov/pubmed/7964399
71. Hamner, S.R., Seth, A., Delp, S.L.: Muscle contributions to propulsion and support during running. J. Biomech. **43**(14), 2709–16 (2010). doi:10.1016/j.jbiomech.2010.06.025. http://www.pubmedcentral.nih.gov/articlerender.fcgi?artid=2973845&tool=pmcentrez&rendertype=abstract
72. Haselgrove, J., Huxley, H.: X-ray evidence for radial cross-bridge movement and for the sliding filament model in actively contracting skeletal muscle. J. Mol. Biol. **77**(4), 549–568 (1973). doi:10.1016/0022-2836(73)90222–2. http://www.sciencedirect.com/science/article/pii/0022283673902222
73. Hatze, H.: A myocybernetic control model of skeletal muscle. Biol. Cybern. **25**(2), 103–119 (1977). doi:10.1007/BF00337268. http://link.springer.com/10.1007/BF00337268
74. Hill, A.: The heat of shortening and the dynamic constants of muscle. Proc. R. Soc. Lond. Ser. B Biol. Sci. **126**(843), 136–195 (1938). http://www.jstor.org/discover/10.2307/82135?uid=2&uid=4&sid=21104544340881
75. Hinder, M.R., Milner, T.E.: The case for an internal dynamics model versus equilibrium point control in human movement. J. Physiol. **549**(Pt 3), 953–63 (2003). doi:10.1113/jphysiol.2002.033845. http://www.pubmedcentral.nih.gov/articlerender.fcgi?artid=2342993&tool=pmcentrez&rendertype=abstract
76. Ivanenko, Y.P., Poppele, R.E., Lacquaniti, F.: Five basic muscle activation patterns account for muscle activity during human locomotion. J. Physiol. **556**(Pt 1), 267–82 (2004). doi:10.1113/jphysiol.2003.057174. http://jp.physoc.org/content/556/1/267.abstract
77. Kamen, G., Gabriel, D.: Essentials of Electromyography. Human Kinetics, Champaign (2010)
78. van der Krogt, M.M., Delp, S.L., Schwartz, M.H.: How robust is human gait to muscle weakness? Gait Posture **36**(1), 113–9 (2012). doi:10.1016/j.gaitpost.2012.01.017. http://www.ncbi.nlm.nih.gov/pubmed/22386624
79. Kutch, J.J., Valero-Cuevas, F.J.: Challenges and new approaches to proving the existence of muscle synergies of neural origin. PLoS Comput. Biol. **8**(5), e1002,434 (2012). doi:10.1371/journal.pcbi.1002434. http://dx.plos.org/10.1371/journal.pcbi.1002434
80. Latash, M.: Motor Control. In Search of Physics of the Living Systems. J. Hum. Kinet. **24**(-1), 7–18 (2010). doi:10.2478/v10078-010-0015-4. http://www.degruyter.com/view/j/hukin.2010.24.issue-1/v10078-010-0015-4/v10078-010-0015-4.xml
81. Latash, M.L.: The bliss (not the problem) of motor abundance (not redundancy). Exp. Brain Res. **217**(1), 1–5 (2012). doi;10.1007/s00221-012-3000-4. http://www.pubmedcentral.nih.gov/articlerender.fcgi?artid=3532046&tool=pmcentrez&rendertype=abstract
82. Lee, D.D., Seung, H.S.: Algorithms for Non-negative Matrix Factorization. In: Advances in Neural Information Processing Systems, pp. 556–562 (2001). http://papers.nips.cc/paper/1861-algorithms-for-non-negative-matrix-factorization
83. Lehman, G.J., McGill, S.M.: The importance of normalization in the interpretation of surface electromyography: a proof of principle. J. Manipulative Physiol. Ther. **22**(7), 444–6 (1999). http://www.ncbi.nlm.nih.gov/pubmed/10519560
84. Levin, M.F., Feldman, A.G.: The role of stretch reflex threshold regulation in normal and impaired motor control. Brain Res. **657**(1–2), 23–30 (1994). http://www.ncbi.nlm.nih.gov/pubmed/7820623
85. Levin, M.F., Lamarre, Y., Feldman, A.G.: Control variables and proprioceptive feedback in fast single-joint movement. Can. J. Physiol. Pharmacol. **73**(2), 316–30 (1995). http://www.ncbi.nlm.nih.gov/pubmed/7621370
86. Liu, M.Q., Anderson, F.C., Pandy, M.G., Delp, S.L.: Muscles that support the body also modulate forward progression during walking. J. Biomech. **39**(14), 2623–30 (2006). doi:10.1016/j.jbiomech.2005.08.017. http://www.ncbi.nlm.nih.gov/pubmed/16216251
87. Liu, M.Q., Anderson, F.C., Schwartz, M.H., Delp, S.L.: Muscle contributions to support and progression over a range of walking speeds. J. Biomech. **41**(15), 3243–52 (2008). doi:10.1016/j.jbiomech.2008.07.031. http://www.ncbi.nlm.nih.gov/pubmed/18822415

88. Lloyd, D.G., Besier, T.F.: An EMG-driven musculoskeletal model to estimate muscle forces and knee joint moments in vivo. J. Biomech. **36**(6), 765–76 (2003). http://www.ncbi.nlm.nih.gov/pubmed/12742444
89. Lloyd, D.G., Besier, T.F., Winby, C.R., Buchanan, T.S.: Neuromusculoskeletal modelling and simulation of tissue load in the lower extremities (2008)
90. Lloyd, D.G., Buchanan, T.S.: A model of load sharing between muscles and soft tissues at the human knee during static tasks. J. Biomech. Eng. **118**(3), 367–76 (1996). http://www.ncbi.nlm.nih.gov/pubmed/8872259
91. Manal, K., Buchanan, T.S.: A one-parameter neural activation to muscle activation model: estimating isometric joint moments from electromyograms. J. Biomech. **36**(8), 1197–202 (2003). http://www.ncbi.nlm.nih.gov/pubmed/12831746
92. Manal, K., Gonzalez, R.V., Lloyd, D.G., Buchanan, T.S.: A real-time EMG-driven virtual arm. Comput. Biol. Med. **32**(1), 25–36 (2002). http://www.ncbi.nlm.nih.gov/pubmed/11738638
93. McGowan, C., Neptune, R., Clark, D., Kautz, S.: Modular control of human walking: adaptations to altered mechanical demands. J. Biomech. **43**(3), 412–419 (2010)
94. McKay, J.L., Ting, L.H.: Functional muscle synergies constrain force production during postural tasks. J. Biomech. **41**(2), 299–306 (2008). doi:10.1016/j.jbiomech.2007.09.012. http://www.ncbi.nlm.nih.gov/pubmed/17980370
95. Menegaldo, L.L., de Toledo Fleury, A., Weber, H.I.: Moment arms and musculotendon lengths estimation for a three-dimensional lower-limb model. J. Biomech. **37**(9), 1447–53 (2004). doi:10.1016/j.jbiomech.2003.12.017. http://www.ncbi.nlm.nih.gov/pubmed/15275854
96. Merletti, R., Di Torino, P.: ISEK standards for reporting EMG data. J. Electromyogr. Kinesiol. **9**(1), 3–4 (1999). http://www.isek-online.org/standards_emg.html
97. Millard, M., Uchida, T., Seth, A., Delp, S.L.: Flexing computational muscle: modeling and simulation of musculotendon dynamics. J. Biomech. Eng. **135**(2), 021,005 (2013). doi:10.1115/1.4023390
98. Milner-Brown, H., Stein, R., Yemm, R.: The orderly recruitment of human motor units during voluntary isometric contractions. J. Physiol. **230**(2), 359 (1973)
99. Milner-Brown, H.S., Stein, R.B., Yemm, R.: The orderly recruitment of human motor units during voluntary isometric contractions. J. Physiol. **230**(2), 359–70 (1973). http://www.pubmedcentral.nih.gov/articlerender.fcgi?artid=1350367&tool=pmcentrez&rendertype=abstract
100. Mndez, J., Keys, A.: Density and composition of mammalian muscle. Metabolism **9**, 184–188 (1960)
101. Nagano, A., Komura, T., Fukashiro, S., Himeno, R.: Force, work and power output of lower limb muscles during human maximal-effort countermovement jumping. J. Electromyogr. Kinesiol. Off. J. Int. Soc. Electrophysiol. Kinesiol. **15**(4), 367–76 (2005). doi:10.1016/j.jelekin.2004.12.006. http://www.ncbi.nlm.nih.gov/pubmed/15811607
102. Neptune, R., Clark, D., Kautz, S.: Modular control of human walking: a simulation study. J. Biomech. **42**(9), 1282–1287 (2009)
103. Nichols, T.R.: Musculoskeletal mechanics: a foundation of motor physiology. Adv. Exp. Med. Biol. **508**, 473–9 (2002). http://www.ncbi.nlm.nih.gov/pubmed/12171145
104. Orlovsky, G.N.: Activity of vestibulospinal neurons during locomotion. Brain Res. **46**, 85–98 (1972). http://www.ncbi.nlm.nih.gov/pubmed/4635375
105. Ostry, D.J., Feldman, A.G.: A critical evaluation of the force control hypothesis in motor control. Exp. Brain Res. **153**(3), 275–88 (2003). doi:10.1007/s00221-003-1624-0. http://www.ncbi.nlm.nih.gov/pubmed/14610628
106. Pandy, M.G., Andriacchi, T.P.: Muscle and joint function in human locomotion. Ann. Rev. Biomed. Eng. **12**, 401–33 (2010). doi:10.1146/annurev-bioeng-070909-105259. http://www.ncbi.nlm.nih.gov/pubmed/20617942
107. Pastor, P., Kalakrishnan, M., Chitta, S., Theodorou, E., Schaal, S.: Skill learning and task outcome prediction for manipulation. In: 2011 IEEE International Conference on Robotics and Automation, pp. 3828–3834. IEEE (2011). doi:10.1109/ICRA.2011.5980200. http://ieeexplore.ieee.org/articleDetails.jsp?arnumber=5980200

108. Patla, A.E.: Understanding the roles of vision in the control of human locomotion. Gait Posture **5**(1), 54–69 (1997). doi:10.1016/S0966-6362(96)01109–5. http://www.sciencedirect.com/science/article/pii/S0966636296011095
109. Prilutsky, B.I., Zatsiorsky, V.M.: Optimization-based models of muscle coordination. Exerc. Sport Sci. Rev. **30**(1), 32–8 (2002). http://www.pubmedcentral.nih.gov/articlerender.fcgi?artid=2821033&tool=pmcentrez&rendertype=abstract
110. Radu, V.: Application. In: Radu, V. (ed.) Stochastic Modeling of Thermal Fatigue Crack Growth. ACM, vol. 1, pp. 63–70. Springer, Heidelberg (2015)
111. Santello, M., Baud-Bovy, G., Jörntell, H.: Neural bases of hand synergies. Front. Comput. Neurosci. **7**, 23 (2013). doi:10.3389/fncom.2013.00023. http://www.pubmedcentral.nih.gov/articlerender.fcgi?artid=3619124&tool=pmcentrez&rendertype=abstract
112. Sartori, M., Gizzi, L., Lloyd, D., Farina, D.: A musculoskeletal model of human locomotion driven by a low dimensional set of impulsive excitation primitives. Front. Comput. Neurosci. **7**, 79 (2013)
113. Sartori, M., Reggiani, M., van den Bogert, A.J., Lloyd, D.G.: Estimation of musculotendon kinematics in large musculoskeletal models using multidimensional B-splines. J. Biomech. **45**(3), 595–601 (2012). doi:10.1016/j.jbiomech.2011.10.040. http://www.sciencedirect.com/science/article/pii/S0021929011006828
114. Scheys, L., Desloovere, K., Suetens, P., Jonkers, I.: Level of subject-specific detail in musculoskeletal models affects hip moment arm length calculation during gait in pediatric subjects with increased femoral anteversion. J. Biomech. **44**(7), 1346–53 (2011). doi:10.1016/j.jbiomech.2011.01.001. http://www.ncbi.nlm.nih.gov/pubmed/21295307
115. Scheys, L., Spaepen, A., Suetens, P., Jonkers, I.: Calculated moment-arm and muscle-tendon lengths during gait differ substantially using MR based versus rescaled generic lower-limb musculoskeletal models. Gait posture **28**(4), 640–8 (2008). doi:10.1016/j.gaitpost.2008.04.010. http://www.ncbi.nlm.nih.gov/pubmed/18534855
116. Schmidt, R.A.: A schema theory of discrete motor skill learning. Psychol. Rev. **82**(4), 225–260 (1975). doi:10.1037/h0076770
117. Schutte, L.M.: Using Musculoskeletal Models to Explore Strategies for Improving Performance in Electrical Stimulation-induced Leg Cycle Ergometry (1993). http://books.google.fr/books/about/Using_Musculoskeletal_Models_to_Explore.html?hl=fr&id=UWnItgAACAAJ&pgis=1
118. Selbie, W.S., Caldwell, G.E.: A simulation study of vertical jumping from different starting postures. J. Biomech. **29**(9), 1137–46 (1996). http://www.ncbi.nlm.nih.gov/pubmed/8872270
119. Seth, A., Sherman, M., Reinbolt, J.A., Delp, S.L.: OpenSim: a musculoskeletal modeling and simulation framework for in silico investigations and exchange. Procedia IUTAM **2**, 212–232 (2011). doi:10.1016/j.piutam.2011.04.021. http://www.sciencedirect.com/science/article/pii/S2210983811000228
120. Shadmehr, R., Wise, S.P.: The Computational Neurobiology of Reaching and Pointing, mit press edn. (2004). http://www.shadmehrlab.org/book-index.htm
121. Steele, K.M., Seth, A., Hicks, J.L., Schwartz, M.S., Delp, S.L.: Muscle contributions to support and progression during single-limb stance in crouch gait. J. Biomech. **43**(11), 2099–105 (2010). doi:10.1016/j.jbiomech.2010.04.003. http://www.pubmedcentral.nih.gov/articlerender.fcgi?artid=2914221&tool=pmcentrez&rendertype=abstract
122. Tax, A.A.M., van der Gon Denier, J.J., Gielen, C.C.A.M., Kleyne, M.: Differences in central control of m. biceps brachii in movement tasks and force tasks. Exp. Brain Res. **79**(1), 138–142 (1990). doi:10.1007/BF00228882. http://link.springer.com/10.1007/BF00228882
123. Ting, L.H., Chvatal, S.A., Safavynia, S.A., McKay, J.L.: Review and perspective: neuromechanical considerations for predicting muscle activation patterns for movement. Int. J. Numer. Methods Biomed. Eng. **28**(10), 1003–14 (2012). doi:10.1002/cnm.2485. http://www.pubmedcentral.nih.gov/articlerender.fcgi?artid=4121429&tool=pmcentrez&rendertype=abstract
124. Todorov, E.: Optimality principles in sensorimotor control. Nat. Neurosci. **7**(9), 907–15 (2004). doi:10.1038/nn1309. http://www.pubmedcentral.nih.gov/articlerender.fcgi?artid=1488877&tool=pmcentrez&rendertype=abstract

125. Todorov, E., Jordan, M.I.: Optimal feedback control as a theory of motor coordination. Nat. Neurosci. **11**(5), 1226–1235 (2002). doi:10.1038/nn963. http://homes.cs.washington.edu/todorov/papers/TodorovNatNeurosci02.pdf
126. Tresch, M.C., Cheung, V.C.K., D'Avella, A.: Matrix factorization algorithms for the identification of muscle synergies: evaluation on simulated and experimental data sets. J. Neurophysiol. **95**(4), 2199–212 (2006). doi:10.1152/jn.00222.2005. http://www.ncbi.nlm.nih.gov/pubmed/16394079
127. Viceconti, M., Taddei, F., Cristofolini, L., Martelli, S., Falcinelli, C., Schileo, E.: Are spontaneous fractures possible? An example of clinical application for personalised, multiscale neuro-musculo-skeletal modelling. J. Biomech. **45**(3), 421–6 (2012). doi:10.1016/j.jbiomech.2011.11.048. http://www.ncbi.nlm.nih.gov/pubmed/22204893
128. Viceconti, M., Taddei, F., Van Sint Jan, S., Leardini, A., Cristofolini, L., Stea, S., Baruffaldi, F., Baleani, M.: Multiscale modelling of the skeleton for the prediction of the risk of fracture. Clin. Biomech. (Bristol, Avon) **23**(7), 845–52 (2008). doi:10.1016/j.clinbiomech.2008.01.009. http://www.ncbi.nlm.nih.gov/pubmed/18304710
129. Winby, C.R., Lloyd, D.G., Kirk, T.B.: Evaluation of different analytical methods for subject-specific scaling of musculotendon parameters. J. Biomech. **41**(8), 1682–1688 (2008)
130. Wing, A.M., Haggard, P., Flanagan, R.J. (eds.): Hand and Brain: The Neurophysiology and Psychology of Hand Movements. Academic Press, San Diego (1996). http://books.google.com/books?id=3p4YIJkz9ygC&pgis=1
131. Winters, J.M., Stark, L.: Muscle models: What is gained and what is lost by varying model complexity. Biol. Cybern. **55**(6), 403–420 (1987). doi:10.1007/BF00318375. http://link.springer.com/10.1007/BF00318375
132. Wolpert, D., Ghahramani, Z.: Computational principles of movement neuroscience. Nat. Neurosci. Suppl. **3**, 1212–1217 (2000). http://www.pubfacts.com/detail/11127840/Computational-principles-of-movement-neuroscience
133. Woods, J.J., Bigland-Ritchie, B.: Linear and non-linear surface EMG/force relationships in human muscles. An anatomical/functional argument for the existence of both. Am. J. Phys. Med. **62**(6), 287–99 (1983). http://www.ncbi.nlm.nih.gov/pubmed/6650674
134. Yamaguchi, G.T., Sawa, A.G.U., Moran, D.W., Fessler, M.J., Winters, J.M.: A survey of human musculotendon actuator parameters. http://www.researchgate.net/publication/239720449_A_survey_of_human_musculotendon_actuator_parameters
135. Zahalak, G.I., Ma, S.P.: Muscle activation and contraction: constitutive relations based directly on cross-bridge kinetics. J. Biomech. Eng. **112**(1), 52–62 (1990). http://www.ncbi.nlm.nih.gov/pubmed/2308304
136. Zajac, F.E.: Muscle and tendon: properties, models, scaling, and application to biomechanics and motor control. Crit. Rev. Biomed. Eng. **17**(4), 359–411 (1989). http://www.ncbi.nlm.nih.gov/pubmed/2676342
137. Zajac, F.E., Neptune, R.R., Kautz, S.A.: Biomechanics and muscle coordination of human walking. Part I: introduction to concepts, power transfer, dynamics and simulations. Gait Posture **16**(3), 215–32 (2002). http://www.ncbi.nlm.nih.gov/pubmed/12443946
138. Zajac, F.E., Neptune, R.R., Kautz, S.A.: Biomechanics and muscle coordination of human walking: part II: lessons from dynamical simulations and clinical implications. Gait Posture **17**(1), 1–17 (2003). http://www.ncbi.nlm.nih.gov/pubmed/12535721